Global fit to $b \to c\tau\nu$ anomalies 2022 mid-autumn

Syuhei Iguro,[(a,b)] **Teppei Kitahara,**[(c,d,e,f)] **and Ryoutaro Watanabe**[(g)]

[(a)] *Institute for Theoretical Particle Physics (TTP), Karlsruhe Institute of Technology (KIT), Engesserstraße 7, 76131 Karlsruhe, Germany*

[(b)] *Institute for Astroparticle Physics (IAP), KIT, Hermann-von-Helmholtz-Platz 1, 76344 Eggenstein-Leopoldshafen, Germany*

[(c)] *Institute for Advanced Research, Nagoya University, Nagoya 464–8601, Japan*

[(d)] *Kobayashi-Maskawa Institute for the Origin of Particles and the Universe, Nagoya University, Nagoya 464–8602, Japan*

[(e)] *KEK Theory Center, IPNS, KEK, Tsukuba 305–0801, Japan*

[(f)] *CAS Key Laboratory of Theoretical Physics, Institute of Theoretical Physics, Chinese Academy of Sciences, Beijing 100190, China*

[(g)] *INFN, Sezione di Pisa, Largo B. Pontecorvo 3, 56127 Pisa, Italy*

igurosyuhei@gmail.com, teppeik@kmi.nagoya-u.ac.jp, wryou1985@gmail.com

Dated: October 18, 2022

Abstract

Recently, the LHCb collaboration announced a preliminary result of the test of lepton flavor universality (LFU) in $B \to D^{(*)}$ semi-leptonic decays: $R_D^{\mathrm{LHCb2022}} = 0.441 \pm 0.089$ and $R_{D^*}^{\mathrm{LHCb2022}} = 0.281 \pm 0.030$ based on the LHC Run 1 data. This is the first result of R_D for the LHCb experiment, and its precision is comparable to the other B-factory data. Interestingly, those data prefer the violation of the LFU again. A new world average of the data from the BaBar, Belle, and LHCb collaborations is $R_D = 0.358 \pm 0.027$ and $R_{D^*} = 0.285 \pm 0.013$. Including this new data, we update a circumstance of the $b \to c\tau\overline{\nu}$ measurements and their implications for new physics. Incorporating recent developments for the $B \to D^{(*)}$ form factors in the Standard Model (SM), we observe a 4.1σ deviation from the SM predictions. Our updates also include; model-independent new physics (NP) formulae for the related observables; and the global fittings of parameters for leptoquark scenarios as well as single NP operator scenarios. Furthermore, we show future potential to indirectly distinguish different new physics scenarios with the use of the precise measurements of the polarization observables in $B \to D^{(*)}\tau\overline{\nu}$ at the Belle II and the high-p_T flavored-tail searches at the LHC. We also discuss an impact on the LFU violation in $\Upsilon \to l^+l^-$.

arXiv:2210.10751v2 [hep-ph] 23 Jan 2023

Contents

1   Introduction

The semi-tauonic B-meson decays, $\overline{B} \to D^{(*)}\tau\overline{\nu}$, have been intriguing processes to measure the lepton flavor universality (LFU):

$$R_D \equiv \frac{\mathcal{B}(\overline{B} \to D\,\tau\,\overline{\nu}_\tau)}{\mathcal{B}(\overline{B} \to D\,\ell\,\overline{\nu}_\ell)}\,, \qquad R_{D^*} \equiv \frac{\mathcal{B}(\overline{B} \to D^*\tau\,\overline{\nu}_\tau)}{\mathcal{B}(\overline{B} \to D^*\ell\,\overline{\nu}_\ell)}\,, \tag{1.1}$$

since it has been reported that the measurements by the BaBar [1, 2], Belle [3–7] and LHCb [8–10] collaborations indicate deviations from the Standard Model (SM) predictions, where $\ell = e$, μ for the BaBar/Belle and $\ell = \mu$ for the LHCb. See Table 1 for the present summary.

A key feature of the deviation is that the measured $R_{D^{(*)}}$ are always *excesses* compared with the SM predictions and thus imply violation of the LFU. Then it has been followed by a ton of theoretical studies to understand its implication from various points of view, *e.g.*, see Ref. [11] and references therein. A confirmation of the LFU violation will provide an evidence of new physics (NP).

1.1   Summary of the current status: 2022 mid-autumn

Three years have passed since the previous experimental report of $R_{D^{(*)}}$ measurements from the B factories [7]. In the meantime, the Belle II experiment finally started taking data

Experiment	R_{D^*}	R_D	Correlation
BaBar [1,2]	$0.332 \pm 0.024 \pm 0.018$	$0.440 \pm 0.058 \pm 0.042$	-0.27
Belle [3]	$0.293 \pm 0.038 \pm 0.015$	$0.375 \pm 0.064 \pm 0.026$	-0.49
Belle [4,5]	$0.270 \pm 0.035^{+0.028}_{-0.025}$	$-$	$-$
Belle [6,7]	$0.283 \pm 0.018 \pm 0.014$	$0.307 \pm 0.037 \pm 0.016$	-0.51
LHCb [9,10]	$0.280 \pm 0.018 \pm 0.029$	$-$	$-$
LHCb [8,18]	$0.281 \pm 0.018 \pm 0.024$	$0.441 \pm 0.060 \pm 0.066$	-0.43
World average [19]	$0.285 \pm 0.010 \pm 0.008$	$0.358 \pm 0.025 \pm 0.012$	-0.29

Table 1. Current status of the independent experimental $R_{D^{(*)}}$ measurements. The first and second errors are statistical and systematic, respectively.

from 2020 [12,13], and the CMS collaboration has developed an innovative data recording method, called "B Parking" since 2019 [14–17], although their official first results are still being awaited.

On the other hand, the LHCb collaboration has shown their results in 2015 and 2017 with the LHCb Run 1 dataset, and thus it was five years passed. Then, now, the LHCb collaboration reported their preliminary result of R_D and also R_{D^*} with the LHCb Run 1 dataset [18],

$$
\begin{aligned}
R_D^{\text{LHCb2022}} &= 0.441 \pm 0.060 \pm 0.066 \,, \\
R_{D^*}^{\text{LHCb2022}} &= 0.281 \pm 0.018 \pm 0.024 \,.
\end{aligned}
\tag{1.2}
$$

The τ is reconstructed in $\tau \to \mu\nu\bar{\nu}$ and the result supersedes the previous result performed in 2015 [8].

In Table 1, we summarize the current status of the $R_{D^{(*)}}$ measurements including the new LHCb result. It is found that the new LHCb result is consistent with the previous world average evaluated in the HFLAV 2021 report [20] within the experimental uncertainty. The combined average of the experimental data gives $p(\chi^2) = 32\%$ with $\chi^2/\text{dof} = 9.21/8$ for the p-value among all data, compared with the previous HFLAV average of 28% with $\chi^2/\text{dof} = 8.8/7$ written in Ref. [20]. The amplified p-value indicates consistency among the data. New world averages of the $R_{D^{(*)}}$ measurements are [19]

$$
\begin{aligned}
R_D &= 0.358 \pm 0.025 \pm 0.012 \,, \\
R_{D^*} &= 0.285 \pm 0.010 \pm 0.008 \,,
\end{aligned}
\tag{1.3}
$$

and R_D–R_{D^*} correlation of -0.29.

Reference	R_D	R_{D^*}	P_τ^D	$-P_\tau^{D^*}$	$F_L^{D^*}$	$R_{J/\psi}$	R_{Λ_c}	$R_{\Upsilon(3S)}$
Bernlochner, *et al.* [22]	0.288(4)	0.249(3)	–	–	–	–	–	–
Iguro, Watanabe [23]	0.290(3)	0.248(1)	0.331(4)	0.497(7)	0.464(3)	–	–	–
Bordone, *et al.* [24,25]	0.298(3)	0.250(3)	0.321(3)	0.492(13)	0.467(9)	–	–	–
HFLAV2021 [20]	0.298(4)	0.254(5)	–	–	–	–	–	–
Refs. [26–28]	–	–	–	–	–	0.258(4)	0.324(4)	0.9948
Data	0.358(28)	0.285(13)	–	$0.38\,^{+0.53}_{-0.55}$	0.60(9)	0.71(25)	0.271(72)	0.968(16)

Table 2. Summary of the SM predictions for the $\overline{B} \to D^{(*)}\tau\overline{\nu}$ and related observables. The current combined results of the experimental measurements are also written in the last line. See the main text for the definitions of the observables.

Regarding the combined average, an important analysis is given in Ref. [21]. The authors pointed out that evaluations of the D^{**} distributions in the SM background involve nontrivial correlations that affect the $R_{D^{(*)}}$ measurements. Their sophisticated study shows that the combined $R_{D^{(*)}}$ average is slightly sifted, which is beyond the scope of our work.[#1]

Recent SM predictions for $R_{D^{(*)}}^{\text{SM}}$ have been obtained in Refs. [20,23–25] as summarized in Table 2. The difference of these SM values is mainly due to development of the $\overline{B} \to D^{(*)}$ form factor evaluations both by theoretical studies and experimental fits, whose details can be found in the literature. In our work, we will employ the work of Ref. [23] as explained soon later.

A further concern for the SM evaluation is long-distance QED corrections to $\overline{B} \to D^{(*)}\ell\overline{\nu}$, which remains an open question. They depend on the lepton mass as being of $\mathcal{O}[\alpha \ln(m_\ell/m_B)]$ and hence it could provide a few percent correction to violation of the LFU in the semileptonic processes [29–32]. This will be crucial in future when the Belle II experiment reaches such an accuracy.

In Fig. 1, we show the latest average of the R_D–R_{D^*} along with the several recent SM predictions. A general consensus from the figure is that the deviation of the experimental data from the SM expectations still remains. For instance, applying the SM prediction from {HFLAV2021 [20], Ref. [22], Ref. [23], Refs. [24,25]}, one can see $\{3.2\sigma, 4.0\sigma, 4.1\sigma, 3.6\sigma\}$ deviations corresponding to p-value $= \{1.2 \times 10^{-3}, 6.4 \times 10^{-5}, 4.8 \times 10^{-5}, 2.7 \times 10^{-4}\}$ ($\Delta\chi^2 = \{13.8, 19.3, 19.9, 16.4\}$ for 2 degrees of freedom), respectively.

In addition to these deviations in the LFU measurements, τ- and D^*-polarization observables in $\overline{B} \to D^{(*)}\tau\overline{\nu}$ also provide us important and nontrivial information. This is because these observables can potentially help us to pin down the NP structure that causes these deviations [33–50]. We refer to the τ longitudinal-polarization asymmetry in $\overline{B} \to D^{(*)}\tau\overline{\nu}$ and the fraction of the D^* longitudinal mode in $\overline{B} \to D^*\tau\overline{\nu}$ as $P_\tau^{D^{(*)}}$ and $F_L^{D^*}$, respectively.

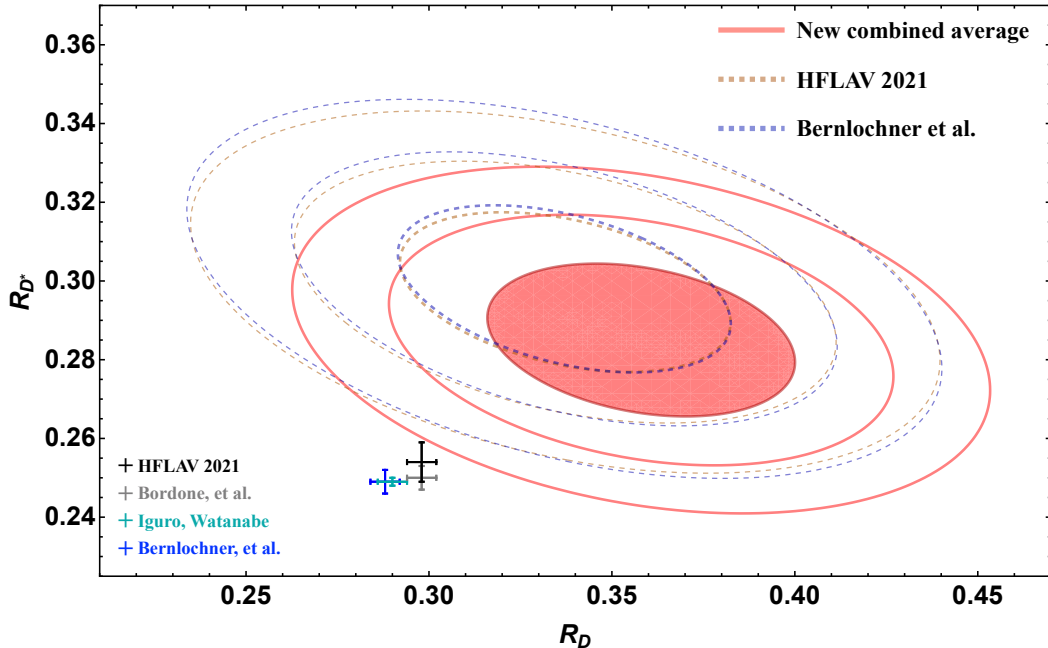[#1]Instead, a comparison among the two previous and new world averages is shown in Fig. 1.

Figure 1. A world average of the latest R_D and R_{D^*} experimental results (red, $1, 2, 3\sigma$ contours), compared with the previous HFLAV 2021 average (dashed orange) [20] and with Ref. [21] (dashed blue) which includes the nontrivial D^{**} contribution. On the other hand, the several SM predictions are shown by crosses [22–25].

See Refs. [42, 51, 52] for their explicit definitions.

In recent years, the first measurements for some of the above polarization observables have been reported by the Belle collaboration. It is summarized as $P_\tau^{D^*} = -0.38 \pm 0.51\,^{+0.21}_{-0.16}$ [4] and $F_L^{D^*} = 0.60 \pm 0.08 \pm 0.04$ [53]. See also Table 2. Although the experimental uncertainty in $F_L^{D^*}$ is still large, this result already has important implications for a tensor-operator NP as pointed out in Ref. [42]. Although P_τ^D is the most striking observable to disentangle the leptoquark (LQ) scenarios that can explain the discrepancy, the experimental study does not exist so far.

Note that the D^* longitudinal polarization in the electron mode has also been measured, $F_L^{D^*}(\overline{B}^0 \to D^{*+}e\overline{\nu}) \equiv F_L^{D^*,e} = 0.56 \pm 0.02$ [53]. This is comparable to the SM prediction of 0.534 ± 0.002 [23]. The $F_L^{D^*}$ and $F_L^{D^*,e}$ measurements have the same level of significance (1.5σ and 1.3σ, respectively).

1.2 Preliminaries of our analysis

Main points of this paper are that (i) we provide state-of-the-art numerical formulae for the observables relevant to the semi-tauonic B decays and (ii) we revisit to perform global fits to the available $R_{D^{(*)}}$ measurements with respect to NP interpretations. It will be given by incorporating following updates and concerns:

- The preliminary result from the LHCb collaboration is encoded in our world average as shown in Table 1.

- The recent development of the $\overline{B} \to D^{(*)}$ transition form factors is taken into account. It is described by the heavy quark effective theory (HQET) taking higher-order corrections up to $\mathcal{O}(\Lambda_{\text{QCD}}^2/m_c^2)$ as introduced in Refs. [24, 54]. We follow the result from the comprehensive theory+experiment fit analysis as obtained in Ref. [23].[#2]

- The recent study of Ref. [22] introduced an approximation method to reduce independent parameters involving the $\mathcal{O}(\Lambda_{\text{QCD}}^2/m_c^2)$ corrections in HQET. Although this affects some of the parameter fits for the form factors, readers can find in Table 2 that our reference values of Ref. [23] are consistent with those of Ref. [22] as for $R_{D^{(*)}}$. Hence we do not take this approximation in our work.

- Recently, Fermilab–MILC Collaborations [55] presented the first lattice result of the form factors for $\overline{B} \to D^*\ell\overline{\nu}$ at nonzero recoil, with which one obtains $R_{D^*}^{\text{SM}} = 0.2484 \pm 0.0013$ and again readers can see the consistency with our reference. Since this preliminary result needs to be finalized and to be compared with upcoming lattice results from the other collaborations such as JLQCD and HPQCD, we do not include this update in our analysis.

- Another way of constraining the form factor has been discussed in Refs. [56–58]. It is free from the parameterization method and obtained by a general property of the unitary bound. They found $R_D^{\text{SM}} = 0.296 \pm 0.008$ and $R_{D^*}^{\text{SM}} = 0.261 \pm 0.020$ ($R_{D^*}^{\text{SM}} = 0.275 \pm 0.021$ by taking the Fermilab–MILC result [55]), slightly larger, but still consistent within the uncertainty. We do not consider this case.

- Indirect LHC bounds from the high-p_T mono-τ searches with large missing transverse energy [59–69] are concerned. We impose the result of Ref. [67] that directly constrains the NP contributions to the $b \to c\tau\overline{\nu}$ current and accounts for the NP-scale dependence on the LHC bound, which is not available by the effective-field-theory description. Requiring an additional b-tagged jet also helps to improve the sensitivity [66, 68]. We will see how it affects the constraints in the leptoquark scenarios.

- Similar sensitivity can be obtained by the $\tau\tau$ final state [70, 71]. It is noted that the about three standard deviation is reported by the CMS collaboration [71], which would imply the existence of leptoquark, while the ATLAS result [70] has not found the similar excess. We need the larger statistics to confirm it, and thus we do not include the constraint to be conservative.

[#2]To be precise, we employ the "(2/1/0) fit" result, preferred by their fit analysis. See the reference for details.

In addition to the above points, we also investigate the following processes that are directly/indirectly related to the $b \to c\tau\overline{\nu}$ current:

- The LFU in $B_c \to J/\psi\, l\, \overline{\nu}$ decays is connected to $R_{D^{(*)}}$. The LHCb collaboration has measured the ratio $R_{J/\psi} \equiv \mathcal{B}(B_c \to J/\psi\, \tau\, \overline{\nu})/\mathcal{B}(B_c \to J/\psi\, \mu\, \overline{\nu}) = 0.71 \pm 0.17 \pm 0.18$ [72]. Although the current data includes such a large uncertainty, it would be useful in future to test some NP scenarios for the sake of the $R_{D^{(*)}}$ anomalies. We update the numerical formula for $R_{J/\psi}$ in the presence of general NP contributions and put a prediction from our fit study.

- The Υ leptonic decays, $\Upsilon \to l^+l^-$, are potentially connected to $R_{D^{(*)}}$ once one specifies NP interactions to the bottom quark and leptons. Although the SM contribution comes from a photon exchange, it is suppressed by the Υ mass squared. The sensitivity to NP is, therefore, not completely negligible, and the LFU of $R_{\Upsilon(nS)} \equiv \mathcal{B}(\Upsilon(nS) \to \tau^+\tau^-)/\mathcal{B}(\Upsilon(nS) \to \ell^+\ell^-)$ can be an important cross check of the $R_{D^{(*)}}$ anomalies. Furthermore, the BaBar collaboration has reported a result which slightly violates the LFU: $R_{\Upsilon(3S)} = 0.966 \pm 0.008 \pm 0.014$ [73]. We investigate the theoretical correlations in several NP models.

This paper is organized as follows. In Sec. 2, we put the numerical formulae for the relevant observables in terms of the effective Hamiltonian. We also summarize the case for single operator analysis. In Sec. 3, based on the generic study with renormalization-group running effects, we obtain relations among R_D, R_{D^*}, and $F_L^{D^*}$ in the LQ models and discuss their potential to explain the present data. Relations to the τ polarizations are also discussed. In Sec. 4, we also investigate the LFU violation in the Υ decays and show its correlation with $b \to c\tau\overline{\nu}$ observables. Finally, we conclude in Sec. 5.

2 General formulae for the observables

At first, we describe general NP contributions to $b \to c\tau\overline{\nu}$ in terms of the effective Hamiltonian. The operators relevant to the processes of interest are described as[#3]

$$\mathcal{H}_{\text{eff}} = 2\sqrt{2}G_F V_{cb}\left[(1 + C_{V_L})O_{V_L} + C_{V_R}O_{V_R} + C_{S_L}O_{S_L} + C_{S_R}O_{S_R} + C_T O_T\right], \quad (2.1)$$

with

$$
\begin{aligned}
O_{V_L} &= (\overline{c}\gamma^\mu P_L b)(\overline{\tau}\gamma_\mu P_L \nu_\tau), & O_{V_R} &= (\overline{c}\gamma^\mu P_R b)(\overline{\tau}\gamma_\mu P_L \nu_\tau), \\
O_{S_L} &= (\overline{c}P_L b)(\overline{\tau}P_L \nu_\tau), & O_{S_R} &= (\overline{c}P_R b)(\overline{\tau}P_L \nu_\tau), \\
O_T &= (\overline{c}\sigma^{\mu\nu}P_L b)(\overline{\tau}\sigma_{\mu\nu}P_L \nu_\tau),
\end{aligned}
\quad (2.2)
$$

[#3]The different naming scheme of the operators are often used [74–76]. Our C_{V_L}, C_{V_R}, C_{S_L}, and C_{S_R} correspond to C_{V_1}, C_{V_2}, C_{S_2}, and C_{S_1}, respectively.

where $P_L = (1 - \gamma_5)/2$ and $P_R = (1 + \gamma_5)/2$. The NP contribution is encoded in the Wilson coefficients (WCs) of C_X, normalized by the SM factor of $2\sqrt{2}G_F V_{cb}$. The SM corresponds to $C_X = 0$ for $X = V_{L,R}$, $S_{L,R}$, and T in this description. We assume that the light neutrino is always left-handed, and NP contributions are relevant to only the third-generation neutrino (ν_τ), for simplicity.[#4]

Note that the leading $SU(2)_L \times U(1)_Y$ invariant operator, to generate the LFU violated type of the O_{V_2} form, is given in dimension-eight as $(\bar{c}_R \gamma^\mu b_R)(\overline{L}^3 \gamma_\mu \tau^A L^3)(\tilde{H}\tau^A H)$. This implies that C_{V_2} in a NP model necessarily has an additional suppression compared with the other operators generated from dimension-six operators. See Ref. [85] for a NP model that can generate the C_{V_2} contributions to $R_{D^{(*)}}$.

In the following parts, the observables for $\overline{B} \to D^{(*)}\tau\overline{\nu}$, $B_c \to \tau\overline{\nu}$, and $B_c \to J/\psi\,\tau\,\overline{\nu}$ are evaluated with Eq. (2.1) at the scale $\mu = \mu_b = 4.18\,\text{GeV}$. The process $\Upsilon(nS) \to l^+l^-$ will be described in detail in Sec. 4.

$\overline{B} \to D^{(*)}\tau\overline{\nu}$

In this work, we follow analytic forms of the differential decay rates for $\overline{B} \to D^{(*)}\tau\overline{\nu}$ obtained in Refs. [74, 86]. Regarding the form factors, we employ the general HQET based description [24], in which the heavy quark expansions [87, 88] are taken up to NLO for $\epsilon_a = \alpha_s/\pi$, $\epsilon_b = \overline{\Lambda}/(2m_b)$ and NNLO for $\epsilon_c = \overline{\Lambda}/(2m_c)$ by recalling the fact $\epsilon_a \sim \epsilon_b \sim \epsilon_c^2$. Thanks to HQET property, the form factors for the different Lorenz structures of the NP operators are connected to that for the SM current, which enables us to evaluate the NP contributions to the observables.

Two parametrization models have been considered with respect to the $z = (\sqrt{w+1} - \sqrt{2})/(\sqrt{w+1} + \sqrt{2})$ expansions for the form factors in this description, with which the most general fit analyses of the form-factor parameters and $|V_{cb}|$ have been performed in Ref. [23]. For the present work, we take the (2/1/0) model with a minor update and apply the updated fit result based on Ref. [23].

We have evaluated the ratio observables, $R_{D^{(*)}}$, $P_\tau^{D^{(*)}}$ and $F_L^{D^*}$, for the case of the effective Hamiltonian of Eq. (2.1) at the scale $\mu = \mu_b$. In the end, we find the following

---

[#4]See Refs. [77–83] for models with the right-handed neutrino ν_R. It is noted that the W' is necessarily accompanied by Z' and thus the recent di-τ resonance search [70, 71] excludes the W_R' explanation [84].

updated numerical formulae,

$$\frac{R_D}{R_D^{\mathrm{SM}}} = |1 + C_{V_L} + C_{V_R}|^2 + 1.01|C_{S_L} + C_{S_R}|^2 + 0.84|C_T|^2$$
$$+ 1.49\mathrm{Re}[(1 + C_{V_L} + C_{V_R})(C_{S_L}^* + C_{S_R}^*)] + 1.08\mathrm{Re}[(1 + C_{V_L} + C_{V_R})C_T^*], \quad (2.3)$$

$$\frac{R_{D^*}}{R_{D^*}^{\mathrm{SM}}} = |1 + C_{V_L}|^2 + |C_{V_R}|^2 + 0.04|C_{S_L} - C_{S_R}|^2 + 16.0|C_T|^2$$
$$- 1.83\mathrm{Re}[(1 + C_{V_L})C_{V_R}^*] - 0.11\mathrm{Re}[(1 + C_{V_L} - C_{V_R})(C_{S_L}^* - C_{S_R}^*)]$$
$$- 5.17\mathrm{Re}[(1 + C_{V_L})C_T^*] + 6.60\mathrm{Re}[C_{V_R}C_T^*], \quad (2.4)$$

$$\frac{P_\tau^D}{P_{\tau,\mathrm{SM}}^D} = \left(\frac{R_D}{R_D^{\mathrm{SM}}}\right)^{-1} \times \left(|1 + C_{V_L} + C_{V_R}|^2 + 3.04|C_{S_L} + C_{S_R}|^2 + 0.17|C_T|^2\right.$$
$$\left. + 4.50\mathrm{Re}[(1 + C_{V_L} + C_{V_R})(C_{S_L}^* + C_{S_R}^*)] - 1.09\mathrm{Re}[(1 + C_{V_L} + C_{V_R})C_T^*]\right), \quad (2.5)$$

$$\frac{P_\tau^{D^*}}{P_{\tau,\mathrm{SM}}^{D^*}} = \left(\frac{R_{D^*}}{R_{D^*}^{\mathrm{SM}}}\right)^{-1} \times \left(|1 + C_{V_1}|^2 + |C_{V_2}|^2 - 0.07|C_{S_1} - C_{S_2}|^2 - 1.85|C_T|^2\right.$$
$$- 1.79\mathrm{Re}[(1 + C_{V_L})C_{V_R}^*] + 0.23\mathrm{Re}[(1 + C_{V_L} - C_{V_R})(C_{S_L}^* - C_{S_R}^*)]$$
$$\left. - 3.47\mathrm{Re}[(1 + C_{V_L})C_T^*] + 4.41\mathrm{Re}[C_{V_R}C_T^*]\right), \quad (2.6)$$

$$\frac{F_L^{D^*}}{F_{L,\mathrm{SM}}^{D^*}} = \left(\frac{R_{D^*}}{R_{D^*}^{\mathrm{SM}}}\right)^{-1} \times \left(|1 + C_{V_L} - C_{V_R}|^2 + 0.08|C_{S_L} - C_{S_R}|^2 + 6.90|C_T|^2\right.$$
$$\left. - 0.25\mathrm{Re}[(1 + C_{V_L} - C_{V_R})(C_{S_L}^* - C_{S_R}^*)] - 4.30\mathrm{Re}[(1 + C_{V_L} - C_{V_R})C_T^*]\right), \quad (2.7)$$

which can be compared with those in the literature [42, 43, 78, 82, 89]. The SM predictions are obtained as[#5]

$$R_D^{\mathrm{SM}} = 0.290 \pm 0.003\,,$$
$$R_{D^*}^{\mathrm{SM}} = 0.248 \pm 0.001\,,$$
$$P_{\tau,\mathrm{SM}}^D = 0.331 \pm 0.004\,, \quad (2.8)$$
$$P_{\tau,\mathrm{SM}}^{D^*} = -0.497 \pm 0.007\,,$$
$$F_{L,\mathrm{SM}}^{D^*} = 0.464 \pm 0.003\,.$$

Furthermore, we have checked uncertainties of the above numerical coefficients in the formulae, based on the fit result from Ref. [23]. The tensor (scalar) terms involve $\sim 4\%$ (10%) uncertainties for the D (D^*) mode, while the others contain less than 1% errors. At present, they are not significant and thus neglected in our following study.

[#5]We updated the fit analysis with the modification of the formula for unitarity bound [87], pointed out by Ref. [90]. It only affects the last digits of the SM predictions, though.

$\underline{B_c \to \tau\overline{\nu}}$

The significant constraint on the scalar operators $O_{S_{L,R}}$ comes from the B_c lifetime measurements (τ_{B_c}) [91–95]: the branching ratio of $B_c^- \to \tau\overline{\nu}$, which has not yet been observed, is significantly amplified by the NP scalar interactions, and the branching ratio is constrained from measured τ_{B_c} [96]. We obtain an upper bound on the WCs as

$$|1 + C_{V_L} - C_{V_R} - 4.35\,(C_{S_L} - C_{S_R})|^2 = \frac{\mathcal{B}(B_c \to \tau\overline{\nu})}{\mathcal{B}(B_c \to \tau\overline{\nu})_{\mathrm{SM}}} < 27.1\left(\frac{\mathcal{B}(B_c \to \tau\overline{\nu})_{\mathrm{UB}}}{0.6}\right), \quad (2.9)$$

with $\mathcal{B}(B_c \to \tau\overline{\nu})_{\mathrm{SM}} \simeq 0.022$. Here, $|V_{cb}| = (41.0 \pm 1.4) \times 10^{-3}$ is used [96]. The b and c quark mass inputs, which are relevant for scalar contributions, are taken as $m_b(\mu_b) = (4.18 \pm 0.03)\,\mathrm{GeV}$ and $m_c(\mu_b) = (0.92 \pm 0.02)\,\mathrm{GeV}$. Reference [92] evaluated that the upper bound (UB) on the branching ratio from τ_{B_c} is $\mathcal{B}(B_c \to \tau\overline{\nu})_{\mathrm{UB}} = 0.3$. However, it is pointed out by Ref. [43] and later confirmed by Ref. [95] that there is a sizeable charm-mass dependence on the B_c decay rate because the dominant contribution comes from the charm-quark decay into strange within the B_c meson. A conservative bound is set by Ref. [43] as $\mathcal{B}(B_c \to \tau\overline{\nu})_{\mathrm{UB}} = 0.6$.

One should note that more aggressive bound $\mathcal{B}(B_c \to \tau\overline{\nu})_{\mathrm{UB}} = 0.1$ has been obtained in Ref. [97] by using LEP data. However, it is pointed out that p_T dependence of the fragmentation function, $b \to B_c$, has been entirely overlooked, and thus the bound must be overestimated by several factors [43, 44, 98]. Although the CEPC and FCC-ee experiments are in planning stages, the future Tera-Z machines can directly measure $\mathcal{B}(B_c \to \tau\overline{\nu})$ at O(1%) level [99, 100].

Thanks to the conservative bound, the left-handed scalar operator, C_{S_L} comes back to the game. For instance a general two-Higgs doublet model is a viable candidate and readers are referred to Refs. [101, 102].

$\underline{B_c \to J/\psi\,\tau\,\overline{\nu}}$

We follow the form factor description from the recent lattice result of Ref. [103] for $B_c \to J/\psi\,\tau\,\overline{\nu}$. We also take $m_b(\mu_b)$ and $m_c(\mu_b)$ for the scalar and tensor sectors as aforementioned. The formula for $R_{J/\psi}$ is given as

$$
\begin{aligned}
\frac{R_{J/\psi}}{R_{J/\psi}^{\mathrm{SM}}} = {}& |1 + C_{V_L}|^2 + |C_{V_R}|^2 + 0.04|C_{S_L} - C_{S_R}|^2 + 14.7|C_T|^2 \\
& - 1.82\mathrm{Re}[(1 + C_{V_L})C_{V_R}^*] - 0.10\mathrm{Re}[(1 + C_{V_L} - C_{V_R})(C_{S_L}^* - C_{S_R}^*)] \\
& - 5.39\mathrm{Re}[(1 + C_{V_L})C_T^*] + 6.57\mathrm{Re}[C_{V_R}C_T^*],
\end{aligned}
\quad (2.10)
$$

where we take $R_{J/\psi}^{\mathrm{SM}} = 0.258 \pm 0.004$ [26]. The coefficients potentially have 10–20% uncertainties for $C_{S_{L,R}}$ and C_T, while a few percent for $C_{V_{L,R}}$.

3 Fit analysis

In this paper, several NP scenarios are investigated in accordance with the following steps:

1. The measurements of R_D, R_{D^*} and $F_L^{D^*}$ are taken in the χ^2 fit, and then the favored regions for the NP parameter space are obtained.

2. We then check whether the above solutions are consistent with the other relevant observables, such as the B_c lifetime and the LHC bound.

3. Furthermore, we evaluate NP predictions on P_τ^D, $P_\tau^{D^*}$ and $R_{J/\psi}$.

4. If applicable, a combined study with $R_{\Upsilon(3S)}$ is discussed.

The χ^2 fit function is defined as

$$\chi^2 \equiv \sum_{i,j} (O^{\text{theory}} - O^{\text{exp}})_i \, \text{Cov}_{ij}^{-1} \, (O^{\text{theory}} - O^{\text{exp}})_j \,, \tag{3.1}$$

where we take into account the $R_{D^{(*)}}$ and $F_L^{D^*}$ measurements for O^{exp} reported by BaBar, LHCb, and Belle collaborations. The covariance is given as $\text{Cov}_{ij} = \Delta O_i^{\text{exp}} \rho_{ij} \Delta O_j^{\text{exp}} + \Delta O_i^{\text{theory}} \delta_{ij} \Delta O_j^{\text{theory}}$, where correlation ρ_{ij} is given as in Table 1 while $\rho_{ij} = \delta_{ij}$ among the independent measurements. For every observables, we have the theory formulae O^{theory} as shown in Sec. 2, and hence obtain best fit values in terms of the WCs as defined in Eq. (2.1).

Given the SM predictions as $R_D^{\text{SM}} = 0.290 \pm 0.003$, $R_{D^*}^{\text{SM}} = 0.248 \pm 0.001$, and $F_{L,\text{SM}}^{D^*} = 0.464 \pm 0.003$, we obtain $\chi_{\text{SM}}^2 = 22.4$ (corresponding to 4.0σ) implying a large deviation from the SM. Recall that this chi-square contains the $F_L^{D^*}$ fit which enlarges the value compared with the $R_{D^{(*)}}$ fit shown in Sec. 1. In order to see how NP scenarios improve the fit, we use "Pull" value (defined in, *e.g.*, Refs. [43, 104]). For cases of the single WC fits, the Pull is equivalent to

$$\text{Pull} \equiv \sqrt{\chi_{\text{SM}}^2 - \chi_{\text{NP-best}}^2} \, (\sigma) \,, \tag{3.2}$$

such that we can discuss quantitative comparisons among the NP scenarios.

Regarding the LHC bound to be compared with the above fit result, we refer to the result from Ref. [67], in which the τ + missing searches have been analyzed. Their result is shown in Table 3, where we give the 95% CL upper limit at the μ_b scale.[#6] It should be emphasized that the LHC bound on the WC has a non-negligible mediator mass dependence, see Ref. [67] for details. This feature is indeed crucial for some NP scenarios as will be seen later. Furthermore it is pointed out that the charge asymmetry of the τ lepton will improve the bound on C_X.

[#6]Note that Table 2 of Ref. [67] shows the LHC bound at $\mu = \Lambda_{\text{LHC}}$.

	$\lvert C_{V_L}\rvert$	$\lvert C_{V_R}\rvert$	$\lvert C_{S_L}\rvert$	$\lvert C_{S_R}\rvert$	$\lvert C_T\rvert$
EFT ($> 10\,\mathrm{TeV}$)	0.32 (0.09)	0.33 (0.09)	0.55 (0.14)	0.55 (0.15)	0.17 (0.04)
LQ ($4\,\mathrm{TeV}$)	0.36 (0.10)	0.40 (0.10)	0.74 (0.17)	0.67 (0.18)	0.22 (0.05)
LQ ($2\,\mathrm{TeV}$)	0.42 (0.12)	0.51 (0.15)	0.80 (0.22)	0.77 (0.22)	0.30 (0.07)

Table 3. The 95% CL upper bounds on the WCs at the $\mu = \mu_b$ scale from the LHC analysis of the $\tau + \text{missing}$ search [67]. The future prospects with b-tagged jet $+ \tau\nu$ final state assuming $3\,\mathrm{ab}^{-1}$ of accumulated data are given in the parenthesis [68]. The NP mass scale is shown as $M_{\mathrm{LQ}} = 2\,\mathrm{TeV}$, $4\,\mathrm{TeV}$ and $\Lambda_{\mathrm{EFT}} > 10\,\mathrm{TeV}$.

3.1 EFT: single operator scenario

We begin with the single NP operator scenarios based on the effective field theory (EFT) of Eq. (2.1). Assuming the WC to be real, we immediately obtain the fit results with the Pull values and predictions of P_τ^D, $P_\tau^{D^*}$ and $R_{J/\psi}$ as shown in Table 4. The allowed regions from the B_c lifetime and current LHC bounds are listed as well.

For all the NP scenarios, we can see much improvement on the fit compared with the SM. A significant change from the previous conclusion (before the new LHCb result [18] came up [44, 105, 106]) is that the C_{S_R} scenario *becomes consistent with the data within 95% CL*, i.e., $\chi^2_{best} < 8.0$ (for three observed data). Furthermore, the $C_{S_R}(\mu_b) \simeq 0.2$ solution indicates the second best Pull. Unfortunately, it is known that the usual type II two-Higgs doublet model (2HDM) cannot achieve this solution because the sign of C_{S_R} must be negative: $C_{S_R} = -m_b m_\tau \tan^2\beta/m_{H^\pm}^2 < 0$. It is noted that even in the generic 2HDM, sizable C_{S_R} contribution is difficult due to constraints from ΔM_s and the LHC search [62, 107]. Instead, the C_{S_L} scenario is likely to explain the present data. This is the same feature with the previous fit result before the LHCb data is included. The C_{V_L} scenario well explains the present data, while C_{V_R} gives a lower Pull. The C_T solution gives unique predictions on the other observables, which may be able to identify the NP scenario, and it predicts a large shift of $F_L^{D^*}$ with opposite direction from the present measurement [42, 53].

Once we allow complex values of WCs, the complex C_{V_R}, C_{S_L}, and C_T scenarios improve the fits such as

$$C_{V_R} \simeq 0.02 \pm i\,0.43 \qquad \text{Pull} = 4.1\,, \tag{3.3}$$

$$C_{S_L} \simeq -0.88 \pm i\,0.88 \qquad \text{Pull} = 4.3\,, \tag{3.4}$$

$$C_T \simeq 0.06 \pm i\,0.16 \qquad \text{Pull} = 3.3\,, \tag{3.5}$$

while the complex C_{V_L} and C_{S_R} scenarios give the same Pulls, compared with those with the real WC scenarios. The complex C_T scenario has a similar Pull with the real C_T case. The complex C_{V_R} result at the above best fit point is, however, not consistent with the LHC

	Pull [χ^2_{best}]	Fitted C_X	Allowed region of C_X		Predictions ($\Delta\chi^2 \leq 1$)		
			$B_c \to \tau\overline{\nu}$	LHC	P_τ^D	$-P_\tau^{D^*}$	$R_{J/\psi}$
SM	$-$ [22.4]	$-$	$-$	$-$	0.331 ± 0.004	0.497 ± 0.007	0.258 ± 0.004
C_{V_L}	4.4 [2.8]	$+0.08(2)$	very loose	$[-0.32, 0.32]$	$[0.331, 0.331]$	$[0.497, 0.497]$	$[0.293, 0.313]$
C_{V_R}	1.9 [18.8]	$-0.05(3)$	very loose	$[-0.33, 0.33]$	$[0.331, 0.331]$	$[0.496, 0.497]$	$[0.271, 0.299]$
C_{S_L}	3.0 [13.3]	$+0.17(5)$	$[-0.94, 1.4]$	$[-0.55, 0.55]$	$[0.440, 0.518]$	$[0.517, 0.533]$	$[0.254, 0.256]$
C_{S_R}	3.8 [7.9]	$+0.20(5)$	$[-1.4, 0.94]$	$[-0.55, 0.55]$	$[0.463, 0.529]$	$[0.454, 0.471]$	$[0.261, 0.263]$
C_T	3.4 [10.6]	$-0.03(1)$	$-$	$[-0.17, 0.17]$	$[0.347, 0.360]$	$[0.459, 0.476]$	$[0.286, 0.309]$

Table 4. The fit results of the single NP operator scenarios assuming real WCs. The WCs are given at the μ_b scale. The allowed ranges of WC from the B_c lifetime and the current LHC bounds are also shown ("very loose" represents very weak bounds). Fitted WCs and predictions of P_τ^D, $P_\tau^{D^*}$ and $R_{J/\psi}$ are in the range of $\Delta\chi^2 = \chi^2 - \chi^2_{\text{best}} \leq 1$.

bound for the case of EFT, $|C_{V_R}| < 0.33$. Nevertheless, it could be relaxed in some LQ models with the mass of the LQ particle to be $M_{\text{LQ}} \gtrsim 2\,\text{TeV}$ as seen in Table 3.

As for the complex C_{S_L} scenario, it looks that the best fit point in Eq. (3.4) is disfavored by the LHC and B_c lifetime constraints. It is noted, however, that the LHC bound is not always proper and depends on the NP model. In the case of the charged Higgs model, for instance, the bound on the s-channel mediator $H^\pm$ significantly depends on the resonant mass. Experimentally it is not easy to probe the low mass $\tau\nu$ resonance due to the huge SM W background. Reference [101] points out that the range of $m_t \leq m_{H^\pm} \leq 400\,\text{GeV}$ is still viable for the 1σ explanation, although LHC Run 2 data is already enough to probe this range if the $\tau\nu + b$ signature is searched [102]. Thus, we leave the LHC bound for the complex C_{S_L} scenario below. Once the B_c bound of eq. (2.9) is imposed, we find

$$C_{S_L} \simeq -0.58 \pm i\,0.88 \qquad \text{Pull} = 4.2\,, \qquad (3.6)$$

for the best Pull within the constraint.

It has been pointed out that q^2 distribution in $\overline{B} \to D^{(*)}\tau\overline{\nu}$ is sensitive to the scalar contribution [86,93]. We do not consider the constraint since the detailed correlation among the bins is not available and the constraints depends on $|V_{cb}|$. Furthermore, experimental analyses for the q^2-distribution measurement rely on the theoretical models [2,3]. In any case, the Belle II data will be important to resolve these issues [76].

In Fig. 2, we show predictions on the plane of P_τ^D–$P_\tau^{D^*}$ from our fit analysis with each complex WC scenario. The allowed regions satisfying $\Delta\chi^2 \leq 1$ (4) are shown in dark (light) orange, brown, and blue for the complex C_{S_L}, C_{S_R}, and C_T scenarios, respectively, where the B_c lifetime and LHC bounds based on the EFT framework are also taken into account. The $C_{V_{L,R}}$ scenarios do not deviate P_τ^D and $P_\tau^{D^*}$ from the SM predictions as shown with the
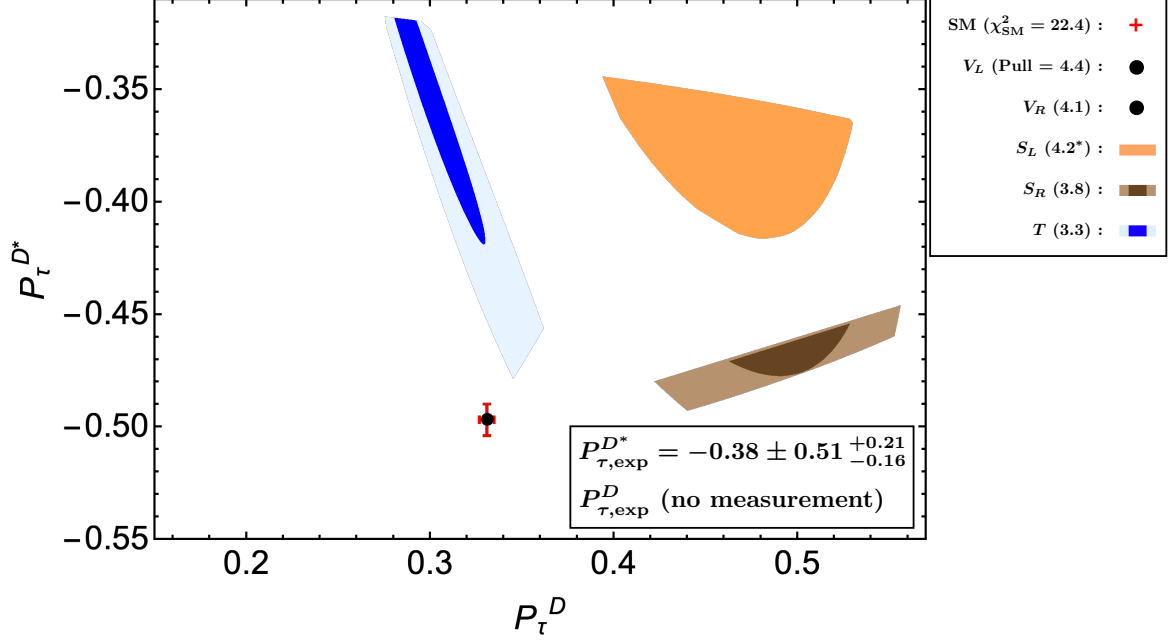
Figure 2. Predictions of P_τ^D and $P_\tau^{D^*}$ in the single complex NP operator scenarios. The allowed regions satisfying $\Delta\chi^2 \leq 1$ (4) are shown in dark (light), orange, brown, and blue for the C_{S_L}, C_{S_R}, and C_T scenarios, respectively, whereas the black dot is the case for the $C_{V_{L,R}}$ scenarios. The B_c lifetime and LHC bounds are also taken into account. As for the S_L scenario, the B_c lifetime rules out the region for $\Delta\chi^2 \leq 1$, whereas the LHC bound is not taken as discussed in the main text.

black dot in the figure. Also note that each shaded region is based on different Pull values, implying different significance, in Fig. 2. We can see that the correlation in τ polarization observables provide the unique predictions that can identify the NP scenarios. On the other hand, $R_{J/\psi}$ is less helpful to distinguish the different operators.

3.2 LQ scenarios

Finally, we study several LQ scenarios. It is well known that three categories of LQs can address the $R_{D^{(*)}}$ anomalies [74], which are referred to as a $SU(2)_L$-singlet vector U_1^μ, a $SU(2)_L$-singlet scalar S_1, and a $SU(2)_L$-doublet scalar R_2. The relevant LQ interactions are given in Appendix A.

A key feature with respect to the fit is that these LQ scenarios involve three independent couplings relevant for $b \to c\tau\nu$, which are encoded in terms of the two independent (and complex in general) WCs as

$$\mathrm{U}_1^\mu : \ C_{V_L} , \ C_{S_R} , \tag{3.7}$$

$$\mathrm{S}_1 : \ C_{V_L} , \ C_{S_L} = -4C_T , \tag{3.8}$$

$$\mathrm{R}_2 : \ C_{V_R} , \ C_{S_L} = 4C_T , \tag{3.9}$$

at the LQ scale $\Lambda_{\mathrm{LQ}} = M_{\mathrm{LQ}}$. The $SU(2)_L$ doublet vector leptoquark V_2 forms C_{S_R} [74], equivalent to the single C_{S_R} scenario, and hence this LQ has now the viable solution as seen in Sec. 3.1. Flavor and collider phenomenologies of V_2 LQ could be interesting, but we leave it for a future work [108].

The C_{V_L} phase in $|1 + C_{V_L}|^2$ can be absorbed [42] in the flavor process. Thus, the absorption of the C_{V_L} phase is irrelevant for the fit within the flavor observables and we take C_{V_L} in U_1 and S_1 LQs as real without loss of generality.[#7] As for C_{V_R} in the R_2 LQ, we assume it as pure imaginary from the fact of Eq. (3.3). Therefore, the three LQ scenarios of our interest have three degrees of freedom for the fit and the relevant observables, and then it is expected that fit results could be different from the previous studies.

These years, UV completions of the LQ scenarios have been studied in the literature; Refs. [109–124] for U_1, Refs. [125–127] for S_1, Refs. [128,129] for R_2, and see also Refs. [130, 131]. In the next subsection, we consider the case if the U_1 LQ is induced by a UV completed theory that gives a specific relation to the LQ couplings, and see how it changes the fit result. Recent re-evaluations on mass differences of the neutral B mesons ΔM_d, ΔM_s, (improved by HQET sum rule and lattice calculations [132]), would constrain a UV-completed TeV-scale LQ model [111,112,124,126,133,134]. In particular, the ratio $\Delta M_d/\Delta M_s$ provides a striking constraint on the coupling texture of the LQ interactions. Here, we comment that a typical UV completion requires a vector-like lepton (VLL) and it induces LQ–VLL box diagrams that contribute to $\Delta M_{d,s}$. This implies that the constraint of our concern depends on the vector-like fermion mass spectrum, and hence we do not consider $\Delta M_{d,s}$ further in our analysis.

The LQ mass has been directly constrained as $M_{\mathrm{LQ}} \gtrsim 1.5\,\mathrm{TeV}$ from the LQ pair production searches [135–137]. Hence we take $M_{\mathrm{LQ}} = 2\,\mathrm{TeV}$ for our benchmark scale. We recap that the WCs are bounded from the τ + missing search and, as shown in Table 3, the LQ scenarios receive milder constraints than the EFT operators as long as $M_{\mathrm{LQ}} \leq 10\,\mathrm{TeV}$.

The WCs will be fitted at the μ_b scale in our analysis, and then they are related to the WCs defined at the $\Lambda_{\mathrm{LQ}} = M_{\mathrm{LQ}}$ scale. The renormalization-group equations (RGEs) (the first matrix below) [138–140] and the LQ-charge independent QCD one-loop matching (the second one) [141] give the following relation

$$
\begin{pmatrix} C_{V_L}(\mu_b) \\ C_{V_R}(\mu_b) \\ C_{S_L}(\mu_b) \\ C_{S_R}(\mu_b) \\ C_T(\mu_b) \end{pmatrix} \simeq \begin{pmatrix} 1 & 0 & 0 & 0 & 0 \\ 0 & 1 & 0 & 0 & 0 \\ 0 & 0 & 1.82 & 0 & -0.35 \\ 0 & 0 & 0 & 1.82 & 0 \\ 0 & 0 & -0.004 & 0 & 0.83 \end{pmatrix} \begin{pmatrix} 1.12 & 0 & 0 & 0 & 0 \\ 0 & 1.07 & 0 & 0 & 0 \\ 0 & 0 & 1.10 & 0 & 0 \\ 0 & 0 & 0 & 1.05 & 0 \\ 0 & 0 & 0 & 0 & 1.07 \end{pmatrix} \begin{pmatrix} C_{V_L}(\Lambda_{\mathrm{LQ}}) \\ C_{V_R}(\Lambda_{\mathrm{LQ}}) \\ C_{S_L}(\Lambda_{\mathrm{LQ}}) \\ C_{S_R}(\Lambda_{\mathrm{LQ}}) \\ C_T(\Lambda_{\mathrm{LQ}}) \end{pmatrix}
$$

[#7]Now the real C_{V_L} fit to the $R_{D^{(*)}}$ anomalies gives the minimum $|C_{V_L}|$, and thus is less constrained from the LHC data.

$$\simeq \begin{pmatrix} 1.12 & 0 & 0 & 0 & 0 \\ 0 & 1.07 & 0 & 0 & 0 \\ 0 & 0 & 1.91 & 0 & -0.38 \\ 0 & 0 & 0 & 2.00 & 0 \\ 0 & 0 & 0. & 0 & 0.89 \end{pmatrix} \begin{pmatrix} C_{V_L}(\Lambda_{\mathrm{LQ}}) \\ C_{V_R}(\Lambda_{\mathrm{LQ}}) \\ C_{S_L}(\Lambda_{\mathrm{LQ}}) \\ C_{S_R}(\Lambda_{\mathrm{LQ}}) \\ C_T(\Lambda_{\mathrm{LQ}}) \end{pmatrix}, \tag{3.10}$$

with $\Lambda_{\mathrm{LQ}} = 2\,\mathrm{TeV}$. Using these numbers, we obtain $C_{S_L}(\mu_b) = -8.9\,C_T(\mu_b)$ and $C_{S_L}(\mu_b) = 8.4\,C_T(\mu_b)$ for S_1 and R_2 LQs, respectively.

With these ingredients, the LQ scenarios in terms of $C_X(\mu_b)$ up to three degrees of freedom are investigated, where the full variable case is referred to as the general LQ. The results of the best fit points for the general LQ scenarios are then summarized as

$$U_1 \text{ LQ}: \qquad C_{V_L} = 0.07\,,\ C_{S_R} = 0.06\,, \qquad\qquad \text{Pull} = 3.8\,, \tag{3.11}$$

$$S_1 \text{ LQ}: \qquad C_{V_L} = 0.06\,,\ C_{S_L} = -8.9\,C_T = 0.06\,, \qquad \text{Pull} = 3.8\,, \tag{3.12}$$

$$R_2 \text{ LQ}: \qquad C_{V_R} = \pm i0.68\,,\ C_{S_L} = 8.4\,C_T = 0.04 \mp i0.65\,, \quad \text{Pull} = 3.8\,. \tag{3.13}$$

We observe that these three general LQ scenarios have the same Pull which means equivalently favored by the current data. We also see that C_{S_R} (C_{S_L}) is preferred to be real at the best fit point for the U_1 (S_1) LQ scenario, whereas C_{S_L} for R_2 LQ is given complex. The fit results for S_1 LQ and R_2 LQ with $C_{V_L} = C_{V_R} = 0$ are obtained as

$$S_1 \text{ LQ } (C_{V_L} = 0): \qquad C_{S_L} = -8.9\,C_T = 0.19\,, \qquad\qquad \text{Pull} = 3.9\,, \tag{3.14}$$

$$R_2 \text{ LQ } (C_{V_R} = 0): \qquad C_{S_L} = 8.4\,C_T = -0.07 \pm i0.58\,, \qquad \text{Pull} = 4.0\,, \tag{3.15}$$

where the improvements of Pull only come from the benefit of reducing the variables.

In turn, we evaluate the LHC bound on the two independent variables, such as (C_{V_L}, C_{S_R}), by the following interpretation

$$U_1 \text{ LQ}: \qquad \frac{|C_{V_L}(\mu_b)|^2}{(0.42)^2} + \frac{|C_{S_R}(\mu_b)|^2}{(0.77)^2} < 1\,, \tag{3.16}$$

$$S_1 \text{ LQ}: \qquad \frac{|C_{V_L}(\mu_b)|^2}{(0.42)^2} + \frac{|C_{S_L}(\mu_b)|^2}{(0.80)^2} < 1\,, \tag{3.17}$$

$$R_2 \text{ LQ}: \qquad \frac{|C_{V_R}(\mu_b)|^2}{(0.51)^2} + \frac{|C_{S_L}(\mu_b)|^2}{(0.80)^2} < 1\,, \tag{3.18}$$

where the denominators are the current LHC bounds for the single WC scenarios with $M_{\mathrm{LQ}} = 2\,\mathrm{TeV}$ from Table 3. Indeed this is a good approximation since the bound comes from the high-p_T region that suppresses the interference term between the $V_{L,R}$ and $S_{L,R}$ operators. It can be seen that the best fit point of Eq. (3.13) for R_2 LQ is not consistent with the LHC bound of Eq. (3.18).

	Pull [χ^2_{best}]	Fitted C_X	Allowed region of C_X		Predictions ($\Delta\chi^2 \leq 1$)		
			$B_c \to \tau\overline{\nu}$	LHC	P_τ^D	$-P_\tau^{D^*}$	$R_{J/\psi}$
SM	$-$ [22.4]	$-$	$-$	$-$	0.331 ± 0.004	0.497 ± 0.007	0.258 ± 0.004
U_1 LQ	3.8 [2.2]	C_{V_L} : $[+0.04, +0.10]$ $\text{Re}C_{S_R}$: $[-0.02, +0.14]$ $\text{Im}C_{S_R}$: $[-0.46, +0.46]$	Eq. (2.9)	Eq. (3.16)	$[0.315, 0.448]$	$[0.474, 0.526]$	$[0.282, 0.309]$
S_1 LQ	3.8 [2.4]	C_{V_L} : $[+0.02, +0.16]$ $\text{Re}C_{S_L}$: $[-0.05, +0.16]$ $\text{Im}C_{S_L}$: $[-0.50, +0.50]$	Eq. (2.9)	Eq. (3.17)	$[0.104, 0.483]$	$[0.373, 0.504]$	$[0.269, 0.311]$
R_2 LQ	3.8 [2.0]	$\text{Im}C_{V_R}$: $[\pm0.00, \pm0.50]$ $\text{Re}C_{S_L}$: $[-0.01, +0.08]$ $\text{Im}C_{S_L}$: $[\mp0.00, \mp0.39]$	Eq. (2.9)	Eq. (3.18)	$[0.286, 0.492]$	$[0.404, 0.537]$	$[0.280, 0.311]$
R_2 LQ ($C_{V_R}=0$)	4.0 [2.8]	$\text{Re}C_{S_L}$: $[-0.13, -0.02]$ $\text{Im}C_{S_L}$: $[\pm0.52, \pm0.65]$	Eq. (2.9)	Eq. (3.18)	$[0.426, 0.500]$	$[0.407, 0.443]$	$[0.276, 0.297]$

Table 5. The fit results of the U_1, S_1, and R_2 LQ scenarios for $M_{\text{LQ}} = 2\,\text{TeV}$. The WCs are given at the μ_b scale. The structure is the same as in Table 4.

In Table 5, we show our fit results and predictions with respect to the LQ scenarios like we did for the EFT cases. It is observed that the general LQ scenarios have less predictive values of the tau polarizations. This can be understood from the fact that the complex scalar WCs give large impacts on the interference terms as can be checked from Eqs. (2.5) and (2.6), which result in the wide ranges of the predictions.

Figure 3 visualizes the combined P_τ^D–$P_\tau^{D^*}$ predictions satisfying $\Delta\chi^2 \leq 1\,(4)$ and the aforementioned bounds, where the general U_1, S_1, and R_2 LQ scenarios are shown in dark (light) green, magenta, and yellow, respectively. The U_1 and R_2 LQ scenarios produce the correlated regions of the P_τ^D–$P_\tau^{D^*}$ predictions and hence could be distinguished. On the other hand, the S_1 LQ scenario has the less-predictive wide region, which is hard to be identified.

Figure 3 also exhibits the predictions for the several specific scenarios, *i.e.*, U_1 LQ with real WC (solid line), S_1 LQ with real WC (dashed line), and R_2 LQ with $C_{V_R} = 0$ (gray region). It is seen that reducing the variable in the general LQ scenario provides the distinct prediction in particular for $P_\tau^{D^*}$ and the correlation for P_τ^D–$P_\tau^{D^*}$ becomes a useful tool to identify the LQ signature. Therefore, it is significant to restrict the LQ interactions by other processes or by a UV theory that realizes the LQ particle. The latter will be discussed in the next subsection for the U_1 LQ (corresponding to the cyan region in the figure). Regarding the S_1 LQ scenario, we comment that a part of the allowed parameter region is ruled out by the $B \to K^*\nu\overline{\nu}$ measurement and ΔM_s (via LQ–ν_τ box) [68].
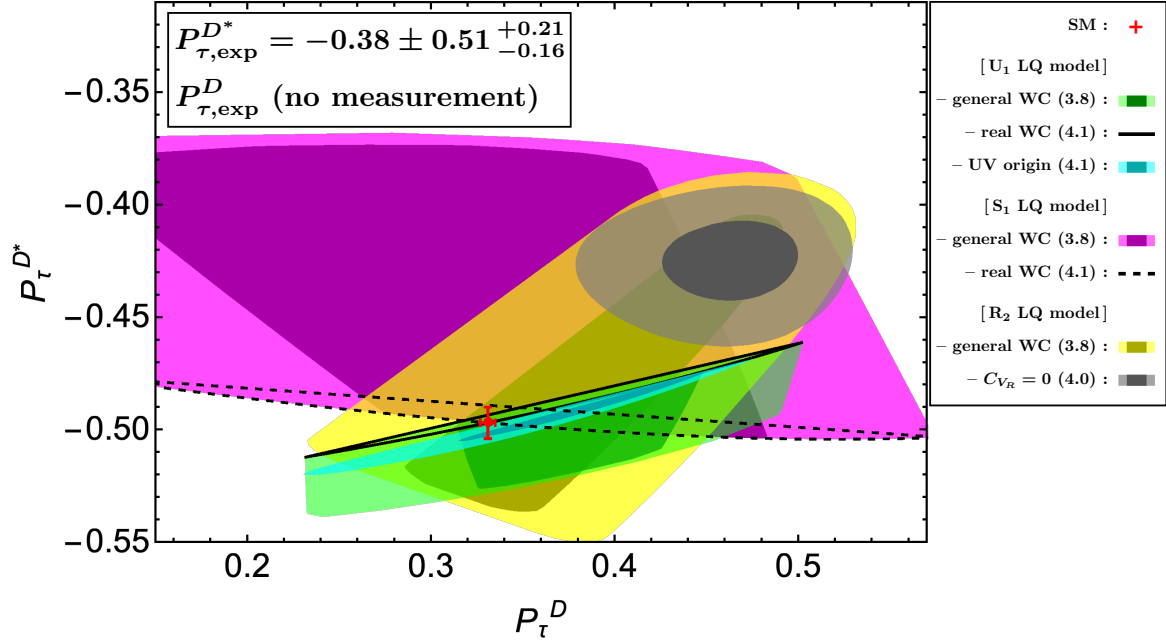
Figure 3. Predictions of P_τ^D and $P_\tau^{D^*}$ in the LQ scenarios following the same procedure as in Fig. 2. The allowed regions are shown in dark (light) green, magenta, and yellow for the general U_1, S_1, and R_2 LQ scenarios, respectively. The specific scenarios; U_1 LQ with UV origin (cyan), real WC (solid line); S_1 LQ with real WC (dashed line); and R_2 LQ with $C_{V_R} = 0$ (gray), are also given.

3.3 UV completion of U_1 LQ

As the U_1 LQ provides a unique solution, not only to the $b \to c\tau\nu$ anomaly, but also to several flavor issues, UV completions of the U_1 LQ have been discussed [142–150]. A typical description is that the U_1 LQ is given as a gauge boson, embedded in a large gauge symmetry, such that the third-generation quarks and leptons are coupled to U_1 in the interaction basis. This means that the two LQ interactions of Eq. (A.1) are represented as a universal gauge coupling, $x_L^{33} = x_R^{33} \equiv g_U$ (see Appendix A). Moving to the mass basis leads to

$$C_{S_R}(\Lambda_{\mathrm{LQ}}) = -2\beta_R \times C_{V_L}(\Lambda_{\mathrm{LQ}})\,, \tag{3.19}$$

where $\beta_R = e^{i\phi}$ denotes the relative complex (CP-violating) phase [149], which comes from the fact that the phases in the rotation matrices (to the mass basis) for quark and lepton are not necessarily identical. The LHC bound for this scenario has been studied and the typical scale of the constraint is obtained as $\Lambda_{\mathrm{LQ}} \gtrsim 3.5\,\mathrm{TeV}$ [111].

The RGE running effect changes the above relation of Eq. (3.19) at the μ_b scale of our interest. By taking $\Lambda_{\mathrm{LQ}} = 4\,\mathrm{TeV}$ as a benchmark scale, we obtain

$$\begin{aligned} C_{V_L}(\mu_b) &= 1 \times 1.11 \times C_{V_L}(\Lambda_{\mathrm{LQ}})\,, \\ C_{S_R}(\mu_b) &= 1.90 \times 1.09 \times C_{S_R}(\Lambda_{\mathrm{LQ}})\,, \end{aligned} \tag{3.20}$$

where the first coefficient is the QCD two-loop RGE factor [140] and the second is the QCD one-loop matching correction [141] at the NP scale. Therefore, we have

$$C_{S_R}(\mu_b) \simeq -3.7 \, \beta_R \times C_{V_L}(\mu_b) \,, \tag{3.21}$$

in the case of the UV origin U_1 LQ scenario, applied to our fit analysis.

The result of the best-fit point for the UV origin U_1 LQ scenario, with the definition of $\beta_R = e^{i\phi}$, is shown as

$$(C_{V_L}, \phi) \simeq (0.07 \,, \pm 0.54\pi) \qquad\qquad \text{Pull} = 4.1 \,. \tag{3.22}$$

One can see that this is consistent with the B_c lifetime and LHC bounds. Predictions of the observables within $\Delta\chi^2 \leq 1,4$ are then given in Fig. 3. It is observed that the large complex phase is favored which suppress the interference. It should be also stressed that the τ polarizations are so unique that this scenario can be distinguished from the aforementioned LQ scenarios.

4 The LFU violation in Υ decays

The UV completed NP models contributing to $b \to c\tau\overline{\nu}$ processes should also bring a related contribution to $b\overline{b} \to \tau^+\tau^-$ or $c\overline{c} \to \tau^+\tau^-$ interactions [28,151,152]. In this section, we show that U_1 and R_2 LQs predict a robust correlation between $b \to c\tau\overline{\nu}$ and $b\overline{b} \to \tau^+\tau^-$ via the LQ exchange.

A definition of the LFU observable in the $\Upsilon(nS)$ decays is

$$R_{\Upsilon(nS)} \equiv \frac{\mathcal{B}(\Upsilon(nS) \to \tau^+\tau^-)}{\mathcal{B}(\Upsilon(nS) \to \ell^+\ell^-)} \,, \tag{4.1}$$

with $n = 1, 2, 3$, where $R_{\Upsilon(nS)} \simeq 1$ holds in the SM. As for $n \geq 4$, the leptonic branching ratios are significantly suppressed since a $B\overline{B}$ decay channel is open.[#8] Since the short- and long-distance QCD corrections [154] are independent of the lepton mass, they are canceled in this ratio. One can also discuss the $c\overline{c} \to l^+l^-$ LFU observable via $\psi(2S)$ decays. However, we do not consider it because the present experimental error is relatively large.

Recently, the BaBar collaboration has reported a precise result for measurement of $R_{\Upsilon(3S)}$ [73]: $R_{\Upsilon(3S)}^{\text{BaBar}} = 0.966 \pm 0.008_{\text{stat}} \pm 0.014_{\text{syst}}$, where $\ell = \mu$. Combing a previous measurement by the CLEO collaboration [155], an average for the $\Upsilon(3S)$ decay is [151]

$$R_{\Upsilon(3S)}^{\text{exp}} = 0.968 \pm 0.016 \,. \tag{4.2}$$

[#8] A novel method for the $n = 4$ mode has been proposed in Ref. [153] by using the inclusive di-leptonic channel $\Upsilon(4S) \to \ell^\pm \tau^\mp X(\overline{\nu}\nu)$, which could be probed in the Belle II experiment and is directly related to $\Gamma(b \to X\tau\nu)/\Gamma(b \to X\ell\nu)$.

This value is consistent with the SM prediction [28]

$$R_{\Upsilon(3S)}^{\mathrm{SM}} = 0.9948 \pm \mathcal{O}(10^{-5}), \tag{4.3}$$

at the 1.7σ level. The SM prediction slightly deviates from 1 whose leading correction comes from the difference in the phase space factor between the τ/ℓ modes [156]. The next-to-leading contribution comes from the QED correction which depends on the lepton mass [157]; $\delta_{\mathrm{EM}}R_{\Upsilon(nS)} = +0.0002$. The tree-level Z exchange also contributes, but its effect is $\mathcal{O}(10^{-5})$ [28]. There is no Higgs boson contribution as one can see below. The other channels ($n = 1, 2$) still suffer from the current experimental uncertainty, and we do not utilize them in our presentation.

The effective Hamiltonian which is relevant to the bottomonium decay into $\tau^+\tau^-$ is described as

$$\begin{aligned}
-\mathcal{H}_{\mathrm{eff}}^{\mathrm{NP}} = {} & C_{VLL}^{b\tau}(\bar{b}\gamma^\mu P_L b)(\bar{\tau}\gamma_\mu P_L \tau) + C_{VRR}^{b\tau}(\bar{b}\gamma^\mu P_R b)(\bar{\tau}\gamma_\mu P_R \tau) \\
& + C_{VLR}^{b\tau}(\bar{b}\gamma^\mu P_L b)(\bar{\tau}\gamma_\mu P_R \tau) + C_{VRL}^{b\tau}(\bar{b}\gamma^\mu P_R b)(\bar{\tau}\gamma_\mu P_L \tau) \\
& + \left[C_T^{b\tau}(\bar{b}\sigma^{\mu\nu} P_R b)(\bar{\tau}\sigma_{\mu\nu} P_R \tau) + C_{SL}^{b\tau}(\bar{b}P_L b)(\bar{\tau}P_L \tau) + C_{SR}^{b\tau}(\bar{b}P_R b)(\bar{\tau}P_L \tau) + \mathrm{h.c.} \right],
\end{aligned} \tag{4.4}$$

at the scale $\mu = m_\Upsilon$. Note that $C_{VLL}^{b\tau}, C_{VRR}^{b\tau}, C_{VLR}^{b\tau}$ and $C_{VRL}^{b\tau}$ are real coefficients, and $C_{SL}^{b\tau}$ and $C_{SR}^{b\tau}$ never contribute to the $\Upsilon(nS) \to \tau^+\tau^-$ due to $\langle 0|\bar{b}b|\Upsilon\rangle = \langle 0|\bar{b}\gamma_5 b|\Upsilon\rangle = 0$. In this convention, the partial decay width is given by [28]

$$\begin{aligned}
\Gamma(\Upsilon(nS) \to \tau^+\tau^-) = {} & \frac{f_\Upsilon^2}{4\pi m_\Upsilon}\sqrt{1 - 4x_\tau^2}\Big[A_\Upsilon^2(1 + 2x_\tau^2) + B_\Upsilon^2(1 - 4x_\tau^2) \\
& + \frac{1}{2}C_\Upsilon^2(1 - 4x_\tau^2)^2 + \frac{1}{2}D_\Upsilon^2(1 - 4x_\tau^2) + 2A_\Upsilon C_\Upsilon x_\tau(1 - 4x_\tau^2) \Big],
\end{aligned} \tag{4.5}$$

with

$$A_\Upsilon = \frac{4\pi\alpha}{3} + \frac{m_\Upsilon^2}{4}\left[C_{VLL}^{b\tau} + C_{VRR}^{b\tau} + C_{VLR}^{b\tau} + C_{VRL}^{b\tau} + 16x_\tau \frac{f_\Upsilon^T}{f_\Upsilon}\mathrm{Re}\left(C_T^{b\tau}\right)\right], \tag{4.6}$$

$$B_\Upsilon = \frac{m_\Upsilon^2}{4}\left(C_{VRR}^{b\tau} + C_{VLR}^{b\tau} - C_{VLL}^{b\tau} - C_{VRL}^{b\tau}\right), \tag{4.7}$$

$$C_\Upsilon = 2m_\Upsilon^2 \frac{f_\Upsilon^T}{f_\Upsilon}\mathrm{Re}\left(C_T^{b\tau}\right), \tag{4.8}$$

$$D_\Upsilon = 2m_\Upsilon^2 \frac{f_\Upsilon^T}{f_\Upsilon}\mathrm{Im}\left(C_T^{b\tau}\right), \tag{4.9}$$

and

$$x_\tau = \frac{m_\tau}{m_\Upsilon}. \tag{4.10}$$

The f_Υ and f_Υ^T are form factors for vector and tensor currents in Υ hadronic-matrix elements, and $f_\Upsilon = f_\Upsilon^T$ holds in the heavy quark limit, which is realized for the Υ decays [28].

Within the SM, this process is predominantly caused by the QED. Nevertheless, the photon-exchange QED contribution is suppressed by $1/m_\Upsilon^2$, and hence the NP contribution could be non-negligible [28, 151, 158]. In the SM, $A_\Upsilon \simeq 4\pi\alpha/3$ and $B_\Upsilon, C_\Upsilon, D_\Upsilon \simeq 0$. Setting the light lepton mass to zero and $m_\Upsilon = m_{\Upsilon(3S)} = 10.355\,\text{GeV}$, we obtain the following numerical formula

$$\frac{R_{\Upsilon(3S)}}{R_{\Upsilon(3S)}^{\text{SM}}} = 1 + 1.64 \times 10^{-3}\,\text{TeV}^2 \left(C_{VLL}^{b\tau} + C_{VRR}^{b\tau} + C_{VLR}^{b\tau} + C_{VRL}^{b\tau} \right)$$
$$+ 6.37 \times 10^{-3}\,\text{TeV}^2\,\text{Re}\left(C_T^{b\tau} \right) + \delta_\Upsilon\,, \tag{4.11}$$

with

$$\delta_\Upsilon = 5.22 \times 10^{-6}\,\text{TeV}^4 \left(C_{VLL}^{b\tau} + C_{VRR}^{b\tau} + C_{VLR}^{b\tau} + C_{VRL}^{b\tau} \right) \text{Re}\left(C_T^{b\tau} \right)$$
$$+ 6.71 \times 10^{-7}\,\text{TeV}^4 \left(C_{VLL}^{b\tau} + C_{VRR}^{b\tau} + C_{VLR}^{b\tau} + C_{VRL}^{b\tau} \right)^2$$
$$+ 5.59 \times 10^{-7}\,\text{TeV}^4 \left(C_{VRR}^{b\tau} + C_{VLR}^{b\tau} - C_{VLL}^{b\tau} - C_{VRL}^{b\tau} \right)^2 \tag{4.12}$$
$$+ 2.51 \times 10^{-5}\,\text{TeV}^4 \left[\text{Re}\left(C_T^{b\tau} \right) \right]^2 + 1.79 \times 10^{-5}\,\text{TeV}^4 \left[\text{Im}\left(C_T^{b\tau} \right) \right]^2\,,$$

where the δ_Υ term gives negligible contributions.

Let us now look into a correlation between $R_{\Upsilon(3S)}$ and $R_{D^{(*)}}$ by using the specific examples of the U_1 and R_2 LQs. First, we exhibit the U_1 LQ case. The U_1 LQ interaction with the SM fermions is given in Eq. (A.1). Integrating the U_1 LQ out, as well as the charged current contributions ($b \to c\tau\bar{\nu}$) in Eq. (A.2), the neutral current ones ($b\bar{b} \to \tau^+\tau^-$) are obtained as

$$C_{VLL}^{b\tau}(\mu_{\text{LQ}}) = -\frac{|x_L^{b\tau}|^2}{m_{U_1}^2}\,, \quad C_{VRR}^{b\tau}(\mu_{\text{LQ}}) = -\frac{|x_R^{b\tau}|^2}{m_{U_1}^2}\,, \quad C_{SR}^{b\tau}(\mu_{\text{LQ}}) = \frac{2x_L^{b\tau}(x_R^{b\tau})^*}{m_{U_1}^2}\,. \tag{4.13}$$

The vector contributions do not change under the RGEs, while the scalar contribution does not affect the Υ decay. Here, an important point is that $R_{\Upsilon(3S)}/R_{\Upsilon(3S)}^{\text{SM}}$ is predicted to be less than 1 when NP contributions are dominated by vector interactions. It would lead to a coherent deviation with $R_{D^{(*)}}$.

Setting $m_{U_1} = 2.0\,\text{TeV}$ and $(Vx_L(\mu_{\text{LQ}}))^{c\tau} = V_{cb}x_L^{b\tau}(\mu_{\text{LQ}})$, namely $x_L^{s\tau}(\mu_{\text{LQ}}) = 0$, we show a correlation between $R_{\Upsilon(3S)}$ and $R_{D^{(*)}}$ in Fig. 4. Here, favored parameter regions in the U_1 LQ model are exhibited on $x_L^{b\tau}$–$x_R^{b\tau}$ plane at the renormalization scale $\mu_{\text{LQ}} = m_{U_1}$. The black contour represents the expected values of $R_{\Upsilon(3S)}$. The red shaded region is favored by $R_{\Upsilon(3S)}^{\text{exp}}$ in Eq. (4.2). It is noted that if we adopt the 2σ constraint of $R_{\Upsilon(3S)}^{\text{exp}}$, the entire parameter region is allowed. The blue and green regions can explain the R_D and R_{D^*} discrepancies within 1σ, respectively. The exclusion region by the LHC analysis ($\tau+$ missing search) is outside the blue line, while the future prospect of the High Luminosity LHC (HL-LHC) is shown by the red dashed line, see Table 3.[#9] Furthermore, the orange dashed line

---

[#9]Note that a stronger collider bound would come from a non-resonant $\tau\tau$ search [70, 71], although it is model-parameter dependent.
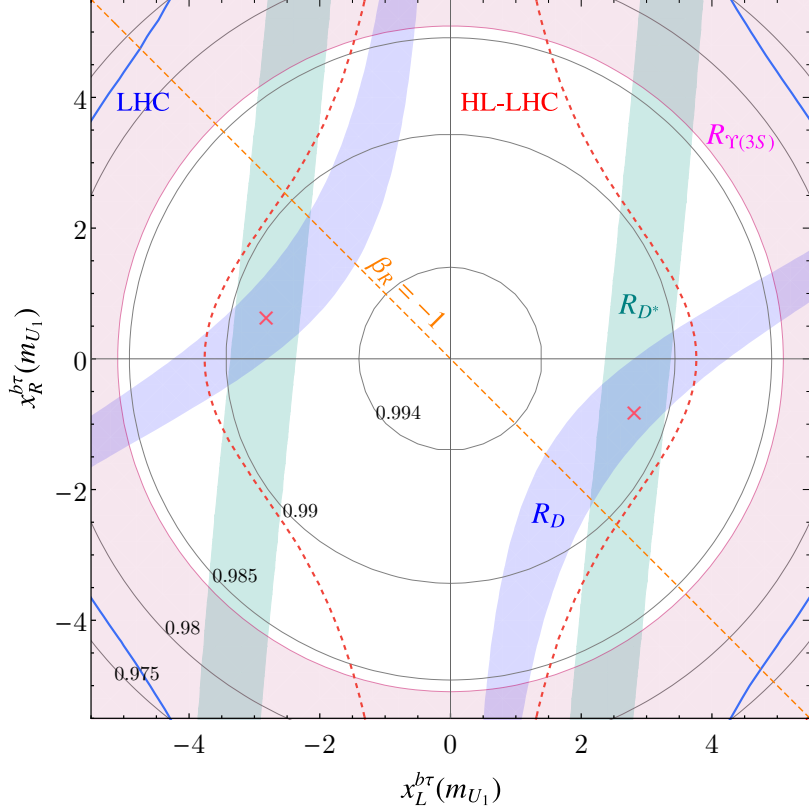
Figure 4. The correlation between $R_{\Upsilon(3S)}$ and $R_{D^{(*)}}$ is exhibited in the U_1 LQ scenario with $m_{U_1} = 2\,\mathrm{TeV}$ by setting $(Vx_L)^{c\tau} = V_{cb}x_L^{b\tau}$. The predicted values of $R_{\Upsilon(3S)}$ are shown by black contours, and $R_{\Upsilon(3S)}^{\mathrm{exp}}$ in Eq. (4.2) is shown in the red shaded area. R_D and R_{D^*} anomalies can be explained in the blue and green regions, respectively. The LHC exclusion region (outside the blue line) and the HL-LHC sensitivity (red dashed line) are based on the result of Table 3. The best fit points of Eq. (3.11) are shown by red crosses. The orange dashed line represents the $U(2)$ flavor symmetry prediction with $\beta_R = -1$.

stands for a prediction in the case of the UV origin U_1 LQ with $\beta_R = -1$ ($\phi = \pi$). From the figure, it is found that the current $R_{\Upsilon(3S)}^{\mathrm{exp}}$ overshoots favored parameter region from the $R_{D^{(*)}}$ anomalies. The best fit points of Eq. (3.11) are shown by red crosses and predict $R_{\Upsilon(3S)} = 0.991$, distinct from the 0.99 contour line in the figure. Thus, it seems crucial to measure $R_{\Upsilon(nS)}$ with less than 1% accuracy in order to distinguish the U_1 LQ signal.

Next, we investigate the R_2 LQ scenario. The R_2 LQ interaction with the SM fermions is given in Eq. (A.6). The generated charged current contributions are given in Eq. (A.7), while the neutral current one is

$$C_{VLR}^{b\tau}(\mu_{\mathrm{LQ}}) = -\frac{|y_R^{b\tau}|^2}{2m_{R_2}^2} \,. \tag{4.14}$$

Since $C_{VLR}^{b\tau} < 0$, $R_{\Upsilon(3S)}/R_{\Upsilon(3S)}^{\mathrm{SM}}$ has to be less than 1 again.

The result is shown in Fig. 5. Here, we set $y_L^{c\tau}(\mu_{\mathrm{LQ}}) = 1$, $|V_{cb}| = 0.04$, and $m_{R_2} =$
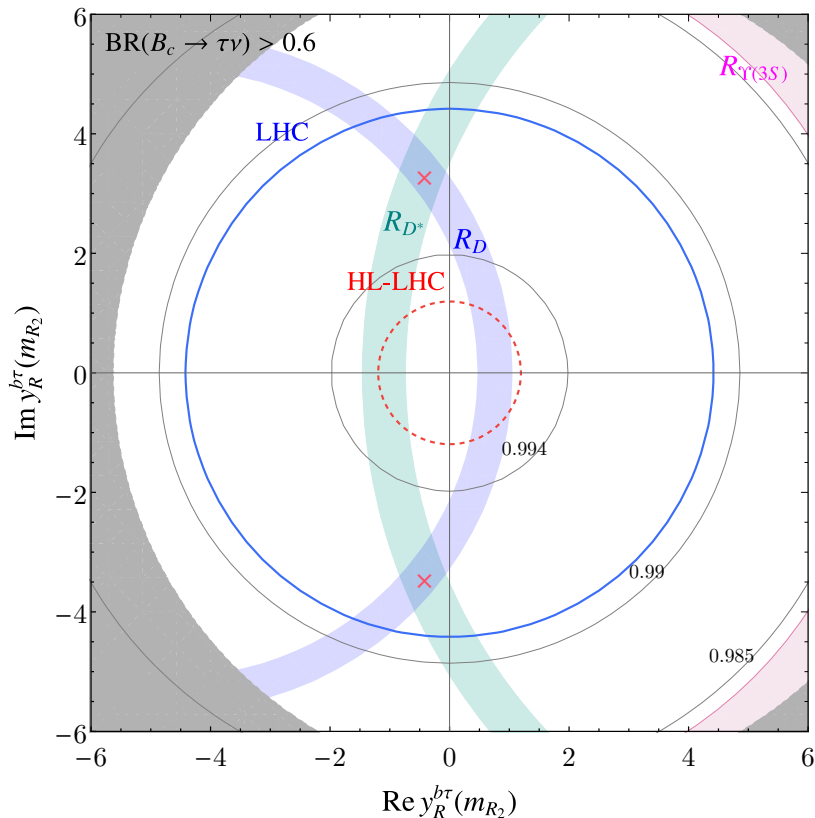
Figure 5. Correlation between $R_{\Upsilon(3S)}$ and $R_{D^{(*)}}$ in the R_2 LQ scenario with $m_{R_2} = 2\,\mathrm{TeV}$ and $y_L^{c\tau} = 1$. The color convention is the same as in Fig. 4. The gray shaded region is excluded by the B_c lifetime. The best fit points of Eq. (3.15) are shown by red crosses.

2.0 TeV, and take $y_R^{b\tau}(\mu_{\mathrm{LQ}})$ as complex value. The color convention is the same as the U_1 LQ case. Furthermore, the gray shaded region is excluded by the B_c lifetime, *i.e.*, $\mathcal{B}(B_c \to \tau\bar{\nu}) > 0.6$. The best fit points in Eq. (3.15) are shown by red crosses, predicting $R_{\Upsilon(3S)} = 0.992$. Similar to U_1 LQ interpretation, 1% accuracy of the $R_{\Upsilon(nS)}$ measurement is required as the R_2 LQ signature.

At the current stage, the large experimental uncertainty in $R_{\Upsilon(3S)}$ cannot allow a clear-cut conclusion. One should note that the Belle and Belle II experiments have enough sensitivities to the $R_{\Upsilon(nS)}$ measurements which would be more accurate than the existing BaBar measurement [159].

5   Conclusions and discussion

In this work we revisited our previous phenomenological investigation and presented a statistical analysis of the LFU violation in $R_{D^{(*)}}$, including the new experimental data from the LHCb experiment. Starting with the re-evaluation of the generic formulae for $R_{D^{(*)}}$ by

	Spin	Charge	Operators	R_D	R_{D^*}	LHC	Flavor
$H^\pm$	0	$(\mathbf{1},\mathbf{2},1/2)$	O_{S_L}	✓	✓	$b\tau\nu$	$B_c \to \tau\nu, F_L^{D^*}, P_\tau^D, M_W$
S_1	0	$(\bar{\mathbf{3}},\mathbf{1},1/3)$	O_{V_L}, O_{S_L}, O_T	✓	✓	$\tau\tau$	$\Delta M_s, P_\tau^D, B \to K^{(*)}\nu\nu$
$R_2^{(2/3)}$	0	$(\mathbf{3},\mathbf{2},7/6)$	$O_{S_L}, O_T, (O_{V_R})$	✓	✓	$b\tau\nu, \tau\tau$	$R_{\Upsilon(nS)}, P_\tau^{D^*}, M_W$
U_1	1	$(\mathbf{3},\mathbf{1},2/3)$	O_{V_L}, O_{S_R}	✓	✓	$b\tau\nu, \tau\tau$	$R_{K^{(*)}}, R_{\Upsilon(nS)}, B_s \to \tau\tau$
$V_2^{(1/3)}$	1	$(\bar{\mathbf{3}},\mathbf{2},5/6)$	O_{S_R}	✓	2σ	$\tau\tau$	$B_s \to \tau\tau, M_W$

Table 6. Summary table for the single-mediator NP scenarios in light of the $b \to c\tau\nu$ anomaly. We add implications for the LHC searches and flavor observables in the last two columns, which is useful to identify the NP scenario. In the $V_2^{(1/3)}$ LQ scenario, 2σ for R_{D^*} implies that it can explain the R_{D^*} anomaly within the 2σ range (but not within 1σ).

employing the recent development of the $B \to D^{(*)}$ transition form factors, we examined the new physics possibility with the low-energy effective Lagrangian as well as the leptoquark models. In addition to the constraints from the low-energy observables and the high-p_T mono-τ search at LHC, the predictions on the relevant observables of R_Υ, $R_{J/\psi}$, and the tau polarizations $P_\tau^{D^{(*)}}$ are evaluated.

To be precise, we performed the χ^2 fit to the experimental measurements of $R_{D^{(*)}}$ and the D^* polarization $F_L^{D^*}$. This updated analysis shows that the present data deviates from the SM predictions at $\sim 4\sigma$ level. Our fit result is summarized in Table 4 with Eqs. (3.3)–(3.5) for the single-operator scenarios, and Table 5 with Eqs. (3.11)–(3.15), (3.22) for the single-mediator leptoquark scenarios. The NP fit improvements compared with the SM one are visualized by Pull as usual, and it was found that the SM-like vector operator still gives the best Pull.

Due to the new LHCb result, the experimental world average has slightly come close to the SM predictions of R_D and R_{D^*}. This change has affected the previous conclusions such that the scalar NP solutions to the $b \to c\tau\nu$ anomaly had been disfavored. Namely, the scalar NP interpretations have been revived now. On the other hand, it is found that the results of the LQ scenarios do not drastically change, compared with the previous fit.

As it was pointed out in the literature, the precise measurements of the polarization observables $P_\tau^{D^{(*)}}$ and $F_L^{D^*}$ have the potential to distinguish the NP scenarios. In Figs. 2 and 3, we show our predictions of P_τ^D and $P_\tau^{D^*}$ for the possible NP scenarios. One can make sure that the single-operator NP scenario explaining the $b \to c\tau\nu$ anomaly can be identified by the $P_\tau^{D^{(*)}}$ measurements, which may be available at the Belle II experiment. On the other hand, the general LQ scenarios are hard to be distinguished due to predicting wide ranges of $P_\tau^{D^{(*)}}$. Once the LQ model with restricted interactions is constructed, however, we see that the $P_\tau^{D^{(*)}}$ measurement has significant potential to probe the LQ signature. The

high energy collider search is also important since the high-p_T lepton search at the LHC can directly probe the NP interactions affecting the LFU ratios.

We also investigated the NP impacts on the LFU violation in the $\Upsilon(nS)$ decays. We found that the LFU ratio R_Υ has to be correlated to $R_{D^{(*)}}$ in the U_1 and R_2 LQ scenarios, while no correlation is expected in the S_1 LQ scenario. It is shown that an experimental accuracy of less than 1% for the $R_{\Upsilon(nS)}$ measurement is necessary in order to identify the LQ scenario. We expect that this is possible in the Belle II experiment.

In Table 6, we put a summary check sheet to find which single-mediator NP scenarios are viable and to see important observables in order to identify the NP scenario responsible for the $b \to c\tau\nu$ anomaly.

Furthermore, it is known that the baryonic counterpart of $R_{D^{(*)}}$, namely $R_{\Lambda_c} \equiv \mathcal{B}(\Lambda_b \to \Lambda_c\,\tau\bar{\nu})/\mathcal{B}(\Lambda_b \to \Lambda_c\,\mu\bar{\nu})$, provides the independent cross check of the $b \to c\tau\nu$ anomaly [43,44]. Recently, R_{Λ_c} has been measured for the first time as $R_{\Lambda_c} = 0.242 \pm 0.026 \pm 0.040 \pm 0.059$ by the LHCb experiment [160], where the last dominant uncertainty comes from an external branching fraction from the LEP measurement [161]. This result implies consistency with the SM prediction at 1.1σ level [27,162], while, instead, normalizing with the SM prediction of $\Gamma(\Lambda_b \to \Lambda_c\mu\bar{\nu})$ improves the accuracy and slightly up-lifts the central value, $e.g.$, $R_{\Lambda_c} = |0.04/V_{cb}|^2(0.285 \pm 0.073)$ [163]. Even though the current experimental uncertainty is not enough precise, it could already provide a nontrivial constraint on the NP parameter space which can explain the $b \to c\tau\nu$ anomaly. An implication of the measured R_{Λ_c} for NP models is given in Ref. [164].

Acknowledgements

A Leptoquark interactions

The LQ interactions are classified with the generic $SU(3)_c \times SU(2)_L \times U(1)_Y$ invariant form [165]. We leave details of the model constructions, and then just introduce the interactions relevant for $b \to c\tau\bar{\nu}$. As mentioned above, there are three viable candidates of leptoquark U_1, S_1, R_2 [166]. Their quantum numbers under $SU(3)_C$, $SU(2)_L$, $U(1)_Y$ are summarized in Table 6.

First, the U_1 vector LQ interaction with the SM fermions, defined in the interaction basis, is given by

$$\mathcal{L}_{U_1} = \hat{x}_L^{ij} \overline{Q}_i \gamma_\mu U_1^\mu L_j + \hat{x}_R^{ij} \overline{d}_{Ri} \gamma_\mu U_1^\mu \ell_{Rj} + \text{h.c.} . \tag{A.1}$$

Integrating out the U_1 LQ mediator particle, then, the Wilson coefficients (WCs) for the charged current of our interest ($b \to c\tau\bar{\nu}$) is obtained as

$$
\begin{aligned}
C_{V_L}(\mu_{\text{LQ}}) &= \frac{1}{2\sqrt{2} G_F V_{cb}} \frac{(V x_L)^{c\tau} (x_L^{b\tau})^*}{m_{U_1}^2} , \\
C_{S_R}(\mu_{\text{LQ}}) &= -\frac{1}{\sqrt{2} G_F V_{cb}} \frac{(V x_L)^{c\tau} (x_R^{b\tau})^*}{m_{U_1}^2} ,
\end{aligned}
\tag{A.2}
$$

where V is the CKM matrix and the couplings $x_{L,R}$ are in the mass basis. The relative sign and factor two in Eq. (A.2) come from the property of Fierz identity.

In a typical UV completed theory [149], the U_1 LQ is realized as a gauge boson generated from a large gauge symmetry and only couples to the third-generation SM fermions. Namely, $\hat{x}_R^{b\tau} = \hat{x}_L^{b\tau} \equiv g_U$, with the others to be zero, is indicated in the gauge interaction basis. Moving to the mass basis, then, generates a non-zero off-diagonal part such as $x_L^{c\tau}$ and also $x_R^{b\tau} = e^{i\phi} x_L^{b\tau}$, where the phase comes from those in the rotation matrices to the mass bases of the left- and right-handed quark and lepton fields that are not canceled in general. Therefore, the UV completion of U_1 LQ suggests

$$C_{S_R}(\mu_{\text{LQ}}) = -2 e^{i\phi} C_{V_L}(\mu_{\text{LQ}}) , \tag{A.3}$$

as introduced in the main text. We also comment that an extension of the fermion families with a nontrivial texture of the fermion mass matrices is necessary to construct a practical UV model [123].

The S_1 scalar LQ interaction in the mass basis is given by

$$\mathcal{L}_{S_1} = \left(V^* y_L\right)^{ij} \overline{u_{Li}^C} \ell_{Lj} S_1 - y_L^{ij} \overline{d_{Li}^C} \nu_{Lj} S_1 + y_R^{ij} \overline{u_{Ri}^C} \ell_{Rj} S_1 + \text{h.c.} . \tag{A.4}$$

In the scalar LQ scenario, the source of the generation violating couplings is off-diagonal element of Yukawa matrices. Then the four-fermion interactions of $b \to c\tau\bar{\nu}$ are given by

$$
\begin{aligned}
C_{S_L}(\mu_{\text{LQ}}) &= -4\, C_T(\mu_{\text{LQ}}) = -\frac{1}{4\sqrt{2} G_F V_{cb}} \frac{y_L^{b\tau} \left(y_R^{c\tau}\right)^*}{m_{S_1}^2} , \\
C_{V_L}(\mu_{\text{LQ}}) &= \frac{1}{4\sqrt{2} G_F V_{cb}} \frac{y_L^{b\tau} \left(V y_L^*\right)^{c\tau}}{m_{S_1}^2} .
\end{aligned}
\tag{A.5}
$$

Finally, we introduce the R_2 scalar LQ interaction. R_2 is a SU(2) doublet and a component with 2/3 of the electromagnetic charge $R_2^{(2/3)}$ can contribute to $b \to c\tau\bar{\nu}$. The Yukawa interaction

$$\mathcal{L}_{R_2} = y_R^{ij}\,\overline{d}_{L\,i}\ell_{R\,j}\,R_2^{(2/3)} + y_L^{ij}\overline{u}_{R\,i}\nu_{L\,j}\,R_2^{(2/3)} + \text{h.c.}\,, \tag{A.6}$$

gives

$$C_{S_L}(\mu_{\mathrm{LQ}}) = 4\,C_T(\mu_{\mathrm{LQ}}) = \frac{1}{4\sqrt{2}G_F V_{cb}}\frac{y_L^{c\tau}\left(y_R^{b\tau}\right)^*}{m_{R_2}^2}\,. \tag{A.7}$$

In contrast to the above two LQ scenarios, the R_2 LQ does not generate C_{V_L} but C_{V_R}. Thus we could expect solid predictions in polarization and related observables. To generate C_{V_R}, indeed, a large mixing between two distinct R_2 LQ doublet is required to induce a proper electroweak symmetry breaking. See details in Refs. [68, 85].

References

[1] **BaBar** Collaboration, "Evidence for an excess of $\bar{B} \to D^{(*)}\tau^-\bar{\nu}_\tau$ decays," Phys. Rev. Lett. **109** (2012) 101802 [arXiv:1205.5442].

[2] **BaBar** Collaboration, "Measurement of an Excess of $\bar{B} \to D^{(*)}\tau^-\bar{\nu}_\tau$ Decays and Implications for Charged Higgs Bosons," Phys. Rev. D **88** (2013) 072012 [arXiv:1303.0571].

[3] **Belle** Collaboration, "Measurement of the branching ratio of $\bar{B} \to D^{(*)}\tau^-\bar{\nu}_\tau$ relative to $\bar{B} \to D^{(*)}\ell^-\bar{\nu}_\ell$ decays with hadronic tagging at Belle," Phys. Rev. D **92** (2015) 072014 [arXiv:1507.03233].

[4] **Belle** Collaboration, "Measurement of the τ lepton polarization and $R(D^*)$ in the decay $\bar{B} \to D^*\tau^-\bar{\nu}_\tau$," Phys. Rev. Lett. **118** (2017) 211801 [arXiv:1612.00529].

[5] **Belle** Collaboration, "Measurement of the τ lepton polarization and $R(D^*)$ in the decay $\bar{B} \to D^*\tau^-\bar{\nu}_\tau$ with one-prong hadronic τ decays at Belle," Phys. Rev. D **97** (2018) 012004 [arXiv:1709.00129].

[6] **Belle** Collaboration, "Measurement of $\mathcal{R}(D)$ and $\mathcal{R}(D^*)$ with a semileptonic tagging method." arXiv:1904.08794.

[7] **Belle** Collaboration, "Measurement of $\mathcal{R}(D)$ and $\mathcal{R}(D^*)$ with a semileptonic tagging method," Phys. Rev. Lett. **124** (2020) 161803 [arXiv:1910.05864].

[8] **LHCb** Collaboration, "Measurement of the ratio of branching fractions $\mathcal{B}(\bar{B}^0 \to D^{*+}\tau^-\bar{\nu}_\tau)/\mathcal{B}(\bar{B}^0 \to D^{*+}\mu^-\bar{\nu}_\mu)$," Phys. Rev. Lett. **115** (2015) 111803 [arXiv:1506.08614]. [Erratum: Phys.Rev.Lett. 115, 159901 (2015)].

[9] **LHCb** Collaboration, "Measurement of the ratio of the $B^0 \to D^{*-}\tau^+\nu_\tau$ and $B^0 \to D^{*-}\mu^+\nu_\mu$ branching fractions using three-prong τ-lepton decays," Phys. Rev. Lett. **120** (2018) 171802 [arXiv:1708.08856].

[10] **LHCb** Collaboration, "Test of Lepton Flavor Universality by the measurement of the $B^0 \to D^{*-}\tau^+\nu_\tau$ branching fraction using three-prong τ decays," Phys. Rev. D **97** (2018) 072013 [arXiv:1711.02505].

[11] D. London and J. Matias, "B Flavour Anomalies: 2021 Theoretical Status Report," Ann. Rev. Nucl. Part. Sci. **72** (2022) 37–68 [arXiv:2110.13270].

[12] **Belle-II** Collaboration, "First flavor tagging calibration using 2019 Belle II data." arXiv:2008.02707.

[13] **Belle-II** Collaboration, "Snowmass White Paper: Belle II physics reach and plans for the next decade and beyond." arXiv:2207.06307.

[14] G. Landsberg, "B Physics Parking Program in CMS." talk in *20th Annual RDMS CMS Collaboration Conference*, 2018.

[15] **CMS** Collaboration, "Recording and reconstructing 10 billion unbiased b hadron decays in CMS," 2019. https://cds.cern.ch/record/2704495.

[16] R. Bainbridge, "Recording and reconstructing 10 billion unbiased b hadron decays in CMS," EPJ Web Conf. **245** (2020) 01025.

[17] Y. Takahashi, "Indications of new physics beyond the Standard Model in flavor anomalies observed at the LHC experiments." talk in *The Physical Society of Japan 2020 Autumn meeting*, 2020.

[18] **LHCb** Collaboration, "$R(D^*)$ and $R(D)$ with $\tau^- \to \mu^- \nu_\tau \overline{\nu}_\mu$.". https://indico.cern.ch/event/1187939/.

[19] **HFLAV** Collaboration. "Average of $R(D)$ and $R(D^*)$ for End of 2022" at https://hflav-eos.web.cern.ch/hflav-eos/semi/fall22/html/RDsDsstar/RDRDs.html.

[20] **HFLAV** Collaboration, "Averages of b-hadron, c-hadron, and τ-lepton properties as of 2021." arXiv:2206.07501. Average of R_D and R_{D^*} for Spring 2021 at https://hflav-eos.web.cern.ch/hflav-eos/semi/spring21/html/RDsDsstar/RDRDs.html.

[21] F. U. Bernlochner, M. F. Sevilla, D. J. Robinson, and G. Wormser, "Semitauonic b-hadron decays: A lepton flavor universality laboratory," Rev. Mod. Phys. **94** (2022) 015003 [arXiv:2101.08326].

[22] F. U. Bernlochner, *et al.*, "Constrained second-order power corrections in HQET: R(D(*)), —Vcb—, and new physics," Phys. Rev. D **106** (2022) 096015 [`arXiv:2206.11281`].

[23] S. Iguro and R. Watanabe, "Bayesian fit analysis to full distribution data of $\overline{B} \to D^{(*)}\ell\overline{\nu} : |V_{cb}|$ determination and new physics constraints," JHEP **08** (2020) 006 [`arXiv:2004.10208`].

[24] M. Bordone, M. Jung, and D. van Dyk, "Theory determination of $\bar{B} \to D^{(*)}\ell^-\bar{\nu}$ form factors at $\mathcal{O}(1/m_c^2)$," Eur. Phys. J. C **80** (2020) 74 [`arXiv:1908.09398`].

[25] M. Bordone, N. Gubernari, D. van Dyk, and M. Jung, "Heavy-Quark expansion for $\bar{B}_s \to D_s^{(*)}$ form factors and unitarity bounds beyond the $SU(3)_F$ limit," Eur. Phys. J. C **80** (2020) 347 [`arXiv:1912.09335`].

[26] **LATTICE-HPQCD** Collaboration, "$R(J/\psi)$ and $B_c^- \to J/\psi\ell^-\bar{\nu}_\ell$ Lepton Flavor Universality Violating Observables from Lattice QCD," Phys. Rev. Lett. **125** (2020) 222003 [`arXiv:2007.06956`].

[27] F. U. Bernlochner, Z. Ligeti, D. J. Robinson, and W. L. Sutcliffe, "New predictions for $\Lambda_b \to \Lambda_c$ semileptonic decays and tests of heavy quark symmetry," Phys. Rev. Lett. **121** (2018) 202001 [`arXiv:1808.09464`].

[28] D. Aloni, A. Efrati, Y. Grossman, and Y. Nir, "Υ and ψ leptonic decays as probes of solutions to the $R_D^{(*)}$ puzzle," JHEP **06** (2017) 019 [`arXiv:1702.07356`].

[29] S. de Boer, T. Kitahara, and I. Nisandzic, "Soft-Photon Corrections to $\bar{B} \to D\tau^-\bar{\nu}_\tau$ Relative to $\bar{B} \to D\mu^-\bar{\nu}_\mu$," Phys. Rev. Lett. **120** (2018) 261804 [`arXiv:1803.05881`].

[30] S. Calí, S. Klaver, M. Rotondo, and B. Sciascia, "Impacts of radiative corrections on measurements of lepton flavour universality in $B \to D\ell\nu_\ell$ decays," Eur. Phys. J. C **79** (2019) 744 [`arXiv:1905.02702`].

[31] G. Isidori and O. Sumensari, "Optimized lepton universality tests in $B \to V\ell\bar{\nu}$ decays," Eur. Phys. J. C **80** (2020) 1078 [`arXiv:2007.08481`].

[32] M. Papucci, T. Trickle, and M. B. Wise, "Radiative semileptonic $\overline{B}$ decays," JHEP **02** (2022) 043 [`arXiv:2110.13154`].

[33] M. Tanaka and R. Watanabe, "Tau longitudinal polarization in $B \to D\tau\nu$ and its role in the search for charged Higgs boson," Phys. Rev. D **82** (2010) 034027 [`arXiv:1005.4306`].

[34] Y. Sakaki and H. Tanaka, "Constraints on the charged scalar effects using the forward-backward asymmetry on B$^-$→D(*)$\tau\nu^-\tau$," Phys. Rev. D **87** (2013) 054002 [`arXiv:1205.4908`].

[35] M. Duraisamy and A. Datta, "The Full $B \to D^* \tau^- \bar{\nu}_\tau$ Angular Distribution and CP violating Triple Products," JHEP **09** (2013) 059 [arXiv:1302.7031].

[36] M. Duraisamy, P. Sharma, and A. Datta, "Azimuthal $B \to D^* \tau^- \bar{\nu}_\tau$ angular distribution with tensor operators," Phys. Rev. D **90** (2014) 074013 [arXiv:1405.3719].

[37] D. Becirevic, S. Fajfer, I. Nisandzic, and A. Tayduganov, "Angular distributions of $\bar{B} \to D^{(*)} \ell \bar{\nu}_\ell$ decays and search of New Physics," Nucl. Phys. B **946** (2019) 114707 [arXiv:1602.03030].

[38] A. K. Alok, D. Kumar, S. Kumbhakar, and S. U. Sankar, "D^* polarization as a probe to discriminate new physics in $\bar{B} \to D^* \tau \bar{\nu}$," Phys. Rev. D **95** (2017) 115038 [arXiv:1606.03164].

[39] M. A. Ivanov, J. G. Körner, and C.-T. Tran, "Probing new physics in $\bar{B}^0 \to D^{(*)} \tau^- \bar{\nu}_\tau$ using the longitudinal, transverse, and normal polarization components of the tau lepton," Phys. Rev. D **95** (2017) 036021 [arXiv:1701.02937].

[40] P. Colangelo and F. De Fazio, "Scrutinizing $\overline{B} \to D^* (D\pi) \ell^- \overline{\nu}_\ell$ and $\overline{B} \to D^* (D\gamma) \ell^- \overline{\nu}_\ell$ in search of new physics footprints," JHEP **06** (2018) 082 [arXiv:1801.10468].

[41] S. Bhattacharya, S. Nandi, and S. Kumar Patra, "$b \to c \tau \nu_\tau$ Decays: a catalogue to compare, constrain, and correlate new physics effects," Eur. Phys. J. C **79** (2019) 268 [arXiv:1805.08222].

[42] S. Iguro, T. Kitahara, Y. Omura, R. Watanabe, and K. Yamamoto, "D^* polarization vs. $R_{D^{(*)}}$ anomalies in the leptoquark models," JHEP **02** (2019) 194 [arXiv:1811.08899].

[43] M. Blanke, *et al.*, "Impact of polarization observables and $B_c \to \tau \nu$ on new physics explanations of the $b \to c \tau \nu$ anomaly," Phys. Rev. D **99** (2019) 075006 [arXiv:1811.09603].

[44] M. Blanke, *et al.*, "Addendum to "Impact of polarization observables and $B_c \to \tau \nu$ on new physics explanations of the $b \to c \tau \nu$ anomaly"," Phys. Rev. D **100** (2019) 035035 [arXiv:1905.08253].

[45] D. Bečirević, M. Fedele, I. Nišandžić, and A. Tayduganov, "Lepton Flavor Universality tests through angular observables of $\overline{B} \to D^{(*)} \ell \overline{\nu}$ decay modes." arXiv:1907.02257.

[46] D. Hill, M. John, W. Ke, and A. Poluektov, "Model-independent method for measuring the angular coefficients of $B^0 \to D^{*-}\tau^+\nu_\tau$ decays," JHEP **11** (2019) 133 [arXiv:1908.04643].

[47] M. Algueró, S. Descotes-Genon, J. Matias, and M. Novoa-Brunet, "Symmetries in $B \to D^*\ell\nu$ angular observables," JHEP **06** (2020) 156 [arXiv:2003.02533].

[48] B. Bhattacharya, A. Datta, S. Kamali, and D. London, "A measurable angular distribution for $\overline{B} \to D^*\tau^-\overline{v}_\tau$ decays," JHEP **07** (2020) 194 [arXiv:2005.03032].

[49] N. Penalva, E. Hernández, and J. Nieves, "New physics and the tau polarization vector in $b \to c\tau\overline{\nu}_\tau$ decays," JHEP **06** (2021) 118 [arXiv:2103.01857].

[50] N. Penalva, E. Hernández, and J. Nieves, "Visible energy and angular distributions of the charged particle from the τ −decay in $b \to c\tau\,(\mu\overline{\nu}_\mu\nu_\tau, \pi\nu_\tau, \rho\nu_\tau)\,\overline{\nu}_\tau$ reactions," JHEP **04** (2022) 026 [arXiv:2201.05537].

[51] M. Tanaka and R. Watanabe, "New physics in the weak interaction of $\bar{B} \to D^{(*)}\tau\bar{\nu}$," Phys. Rev. D **87** (2013) 034028 [arXiv:1212.1878].

[52] P. Asadi, M. R. Buckley, and D. Shih, "Asymmetry Observables and the Origin of $R_{D^{(*)}}$ Anomalies," Phys. Rev. D **99** (2019) 035015 [arXiv:1810.06597].

[53] **Belle** Collaboration, "Measurement of the D^{*-} polarization in the decay $B^0 \to D^{*-}\tau^+\nu_\tau$." arXiv:1903.03102.

[54] M. Jung and D. M. Straub, "Constraining new physics in $b \to c\ell\nu$ transitions," JHEP **01** (2019) 009 [arXiv:1801.01112].

[55] **Fermilab Lattice, MILC** Collaboration, "Semileptonic form factors for $B \to D^*\ell\nu$ at nonzero recoil from $2 + 1$-flavor lattice QCD." arXiv:2105.14019.

[56] G. Martinelli, S. Simula, and L. Vittorio, "Constraints for the semileptonic $B \to D(*)$ form factors from lattice QCD simulations of two-point correlation functions," Phys. Rev. D **104** (2021) 094512 [arXiv:2105.07851].

[57] G. Martinelli, S. Simula, and L. Vittorio, "$|V_{cb}|$ and $R(D)^{(*)})$ using lattice QCD and unitarity," Phys. Rev. D **105** (2022) 034503 [arXiv:2105.08674].

[58] G. Martinelli, S. Simula, and L. Vittorio, "Exclusive determinations of $|V_{cb}|$ and $R(D^*)$ through unitarity," Eur. Phys. J. C **82** (2022) 1083 [arXiv:2109.15248].

[59] A. Greljo, J. Martin Camalich, and J. D. Ruiz-Álvarez, "Mono-τ Signatures at the LHC Constrain Explanations of B-decay Anomalies," Phys. Rev. Lett. **122** (2019) 131803 [arXiv:1811.07920].

[60] B. Dumont, K. Nishiwaki, and R. Watanabe, "LHC constraints and prospects for S_1 scalar leptoquark explaining the $\bar{B} \to D^{(*)}\tau\bar{\nu}$ anomaly," Phys. Rev. D **94** (2016) 034001 [arXiv:1603.05248].

[61] W. Altmannshofer, P. S. Bhupal Dev, and A. Soni, "$R_{D^{(*)}}$ anomaly: A possible hint for natural supersymmetry with R-parity violation," Phys. Rev. D **96** (2017) 095010 [arXiv:1704.06659].

[62] S. Iguro and K. Tobe, "$R(D^{(*)})$ in a general two Higgs doublet model," Nucl. Phys. B **925** (2017) 560–606 [arXiv:1708.06176].

[63] M. Abdullah, J. Calle, B. Dutta, A. Flórez, and D. Restrepo, "Probing a simplified, W' model of $R(D^{(*)})$ anomalies using b-tags, τ leptons and missing energy," Phys. Rev. D **98** (2018) 055016 [arXiv:1805.01869].

[64] S. Iguro, Y. Omura, and M. Takeuchi, "Test of the $R(D^{(*)})$ anomaly at the LHC," Phys. Rev. D **99** (2019) 075013 [arXiv:1810.05843].

[65] M. J. Baker, J. Fuentes-Martín, G. Isidori, and M. König, "High- p_T signatures in vector–leptoquark models," Eur. Phys. J. C **79** (2019) 334 [arXiv:1901.10480].

[66] D. Marzocca, U. Min, and M. Son, "Bottom-Flavored Mono-Tau Tails at the LHC," JHEP **12** (2020) 035 [arXiv:2008.07541].

[67] S. Iguro, M. Takeuchi, and R. Watanabe, "Testing Leptoquark/EFT in $\bar{B} \to D^{(*)}l\bar{\nu}$ at the LHC," Eur. Phys. J. C **81** (2021) 406 [arXiv:2011.02486].

[68] M. Endo, S. Iguro, T. Kitahara, M. Takeuchi, and R. Watanabe, "Non-resonant new physics search at the LHC for the $b \to c\tau\nu$ anomalies," JHEP **02** (2022) 106 [arXiv:2111.04748].

[69] F. Jaffredo, "Revisiting mono-tau tails at the LHC," Eur. Phys. J. C **82** (2022) 541 [arXiv:2112.14604].

[70] **ATLAS** Collaboration, "Search for heavy Higgs bosons decaying into two tau leptons with the ATLAS detector using pp collisions at $\sqrt{s} = 13$ TeV," Phys. Rev. Lett. **125** (2020) 051801 [arXiv:2002.12223].

[71] **CMS** Collaboration, "Searches for additional Higgs bosons and for vector leptoquarks in $\tau\tau$ final states in proton-proton collisions at $\sqrt{s} = 13$ TeV." arXiv:2208.02717.

[72] **LHCb** Collaboration, "Measurement of the ratio of branching fractions $\mathcal{B}(B_c^+ \to J/\psi\tau^+\nu_\tau)/\mathcal{B}(B_c^+ \to J/\psi\mu^+\nu_\mu)$," Phys. Rev. Lett. **120** (2018) 121801 [arXiv:1711.05623].

[73] **BaBar** Collaboration, "Precision measurement of the $\mathcal{B}(\Upsilon(3S) \to \tau^+\tau^-)/\mathcal{B}(\Upsilon(3S) \to \mu^+\mu^-)$ ratio," Phys. Rev. Lett. **125** (2020) 241801 [arXiv:2005.01230].

[74] Y. Sakaki, M. Tanaka, A. Tayduganov, and R. Watanabe, "Testing leptoquark models in $\bar{B} \to D^{(*)}\tau\bar{\nu}$," Phys. Rev. D **88** (2013) 094012 [arXiv:1309.0301].

[75] Z.-R. Huang, Y. Li, C.-D. Lu, M. A. Paracha, and C. Wang, "Footprints of New Physics in $b \to c\tau\nu$ Transitions," Phys. Rev. D **98** (2018) 095018 [arXiv:1808.03565].

[76] E. Kou and P. Urquijo, eds., "The Belle II Physics Book," PTEP **2019** (2019) 123C01 [arXiv:1808.10567]. [Erratum: PTEP 2020, 029201 (2020)].

[77] S. Iguro and Y. Omura, "Status of the semileptonic B decays and muon g-2 in general 2HDMs with right-handed neutrinos," JHEP **05** (2018) 173 [arXiv:1802.01732].

[78] P. Asadi, M. R. Buckley, and D. Shih, "It's all right(-handed neutrinos): a new W' model for the $R_{D^{(*)}}$ anomaly," JHEP **09** (2018) 010 [arXiv:1804.04135].

[79] A. Greljo, D. J. Robinson, B. Shakya, and J. Zupan, "R(D$^{(*)}$) from W$'$ and right-handed neutrinos," JHEP **09** (2018) 169 [arXiv:1804.04642].

[80] D. J. Robinson, B. Shakya, and J. Zupan, "Right-handed neutrinos and R(D$^{(*)}$)," JHEP **02** (2019) 119 [arXiv:1807.04753].

[81] K. S. Babu, B. Dutta, and R. N. Mohapatra, "A theory of R(D*, D) anomaly with right-handed currents," JHEP **01** (2019) 168 [arXiv:1811.04496].

[82] R. Mandal, C. Murgui, A. Peñuelas, and A. Pich, "The role of right-handed neutrinos in $b \to c\tau\bar{\nu}$ anomalies," JHEP **08** (2020) 022 [arXiv:2004.06726].

[83] N. Penalva, E. Hernández, and J. Nieves, "The role of right-handed neutrinos in $b \to c_\tau(\pi\nu_\tau, \rho\nu_\tau, \mu\bar{\nu}_\mu\nu_\tau)\bar{\nu}_\tau$ from visible final-state kinematics," JHEP **10** (2021) 122 [arXiv:2107.13406].

[84] S. Iguro, S. Mishima, and M. Endo. Private communication.

[85] P. Asadi, *New solutions to the charged current B-anomalies*. PhD thesis, Rutgers U., Piscataway (main), 2019.

[86] Y. Sakaki, M. Tanaka, A. Tayduganov, and R. Watanabe, "Probing New Physics with q^2 distributions in $\bar{B} \to D^{(*)}\tau\bar{\nu}$," Phys. Rev. D **91** (2015) 114028 [arXiv:1412.3761].

[87] I. Caprini, L. Lellouch, and M. Neubert, "Dispersive bounds on the shape of $\bar{B} \to D^{(*)}\ell\bar{\nu}$ form factors," Nucl. Phys. B **530** (1998) 153–181 [`hep-ph/9712417`].

[88] F. U. Bernlochner, Z. Ligeti, M. Papucci, and D. J. Robinson, "Combined analysis of semileptonic B decays to D and D^*: $R(D^{(*)})$, $|V_{cb}|$, and new physics," Phys. Rev. D **95** (2017) 115008 [`arXiv:1703.05330`]. [Erratum: Phys.Rev.D 97, 059902 (2018)].

[89] F. Feruglio, P. Paradisi, and O. Sumensari, "Implications of scalar and tensor explanations of $R_{D^{(*)}}$," JHEP **11** (2018) 191 [`arXiv:1806.10155`].

[90] D. Bigi, P. Gambino, and S. Schacht, "$R(D^*)$, $|V_{cb}|$, and the Heavy Quark Symmetry relations between form factors," JHEP **11** (2017) 061 [`arXiv:1707.09509`].

[91] M. Beneke and G. Buchalla, "The B_c Meson Lifetime," Phys. Rev. D **53** (1996) 4991–5000 [`hep-ph/9601249`].

[92] R. Alonso, B. Grinstein, and J. Martin Camalich, "Lifetime of B_c^- Constrains Explanations for Anomalies in $B \to D^{(*)}\tau\nu$," Phys. Rev. Lett. **118** (2017) 081802 [`arXiv:1611.06676`].

[93] A. Celis, M. Jung, X.-Q. Li, and A. Pich, "Scalar contributions to $b \to c(u)\tau\nu$ transitions," Phys. Lett. B **771** (2017) 168–179 [`arXiv:1612.07757`].

[94] R. Watanabe, "New Physics effect on $B_c \to J/\psi\tau\bar{\nu}$ in relation to the $R_{D^{(*)}}$ anomaly," Phys. Lett. B **776** (2018) 5–9 [`arXiv:1709.08644`].

[95] J. Aebischer and B. Grinstein, "Standard Model prediction of the B_c lifetime," JHEP **07** (2021) 130 [`arXiv:2105.02988`].

[96] **Particle Data Group** Collaboration, "Review of Particle Physics," PTEP **2020** (2020) 083C01.

[97] A. G. Akeroyd and C.-H. Chen, "Constraint on the branching ratio of $B_c \to \tau\bar{\nu}$ from LEP1 and consequences for $R(D^{(*)})$ anomaly," Phys. Rev. D **96** (2017) 075011 [`arXiv:1708.04072`].

[98] D. Bardhan and D. Ghosh, "B -meson charged current anomalies: The post-Moriond 2019 status," Phys. Rev. D **100** (2019) 011701 [`arXiv:1904.10432`].

[99] T. Zheng, *et al.*, "Analysis of $B_c \to \tau\nu_\tau$ at CEPC," Chin. Phys. C **45** (2021) 023001 [`arXiv:2007.08234`].

[100] Y. Amhis, M. Hartmann, C. Helsens, D. Hill, and O. Sumensari, "Prospects for $B_c^+ \to \tau^+\nu_\tau$ at FCC-ee," JHEP **12** (2021) 133 [`arXiv:2105.13330`].

[101] S. Iguro, "Revival of H- interpretation of RD(*) anomaly and closing low mass window," Phys. Rev. D **105** (2022) 095011 [`arXiv:2201.06565`].

[102] M. Blanke, S. Iguro, and H. Zhang, "Towards ruling out the charged Higgs interpretation of the $R_{D^{(*)}}$ anomaly," JHEP **06** (2022) 043 [`arXiv:2202.10468`].

[103] **HPQCD** Collaboration, "$B_c \to J/\psi$ form factors for the full q^2 range from lattice QCD," Phys. Rev. D **102** (2020) 094518 [`arXiv:2007.06957`].

[104] S. Descotes-Genon, L. Hofer, J. Matias, and J. Virto, "Global analysis of $b \to s\ell\ell$ anomalies," JHEP **06** (2016) 092 [`arXiv:1510.04239`].

[105] C. Murgui, A. Peñuelas, M. Jung, and A. Pich, "Global fit to $b \to c\tau\nu$ transitions," JHEP **09** (2019) 103 [`arXiv:1904.09311`].

[106] R.-X. Shi, L.-S. Geng, B. Grinstein, S. Jäger, and J. Martin Camalich, "Revisiting the new-physics interpretation of the $b \to c\tau\nu$ data," JHEP **12** (2019) 065 [`arXiv:1905.08498`].

[107] D. A. Faroughy, A. Greljo, and J. F. Kamenik, "Confronting lepton flavor universality violation in B decays with high-p_T tau lepton searches at LHC," Phys. Lett. B **764** (2017) 126–134 [`arXiv:1609.07138`].

[108] S. Iguro and Y. Omura. Private communication.

[109] L. Di Luzio, A. Greljo, and M. Nardecchia, "Gauge leptoquark as the origin of B-physics anomalies," Phys. Rev. D **96** (2017) 115011 [`arXiv:1708.08450`].

[110] A. Greljo and B. A. Stefanek, "Third family quark–lepton unification at the TeV scale," Phys. Lett. B **782** (2018) 131–138 [`arXiv:1802.04274`].

[111] C. Cornella, J. Fuentes-Martin, and G. Isidori, "Revisiting the vector leptoquark explanation of the B-physics anomalies," JHEP **07** (2019) 168 [`arXiv:1903.11517`].

[112] L. Di Luzio, J. Fuentes-Martin, A. Greljo, M. Nardecchia, and S. Renner, "Maximal Flavour Violation: a Cabibbo mechanism for leptoquarks," JHEP **11** (2018) 081 [`arXiv:1808.00942`].

[113] M. Bordone, C. Cornella, J. Fuentes-Martin, and G. Isidori, "A three-site gauge model for flavor hierarchies and flavor anomalies," Phys. Lett. B **779** (2018) 317–323 [`arXiv:1712.01368`].

[114] M. Bordone, C. Cornella, J. Fuentes-Martín, and G. Isidori, "Low-energy signatures of the PS^3 model: from B-physics anomalies to LFV," JHEP **10** (2018) 148 [`arXiv:1805.09328`].

[115] M. Blanke and A. Crivellin, "B Meson Anomalies in a Pati-Salam Model within the Randall-Sundrum Background," Phys. Rev. Lett. **121** (2018) 011801 [arXiv:1801.07256].

[116] S. Balaji, R. Foot, and M. A. Schmidt, "Chiral SU(4) explanation of the $b \to s$ anomalies," Phys. Rev. D **99** (2019) 015029 [arXiv:1809.07562].

[117] S. Balaji and M. A. Schmidt, "Unified SU(4) theory for the $R_{D^{(*)}}$ and $R_{K^{(*)}}$ anomalies," Phys. Rev. D **101** (2020) 015026 [arXiv:1911.08873].

[118] J. Fuentes-Martín and P. Stangl, "Third-family quark-lepton unification with a fundamental composite Higgs," Phys. Lett. B **811** (2020) 135953 [arXiv:2004.11376].

[119] J. Fuentes-Martín, G. Isidori, M. König, and N. Selimović, "Vector Leptoquarks Beyond Tree Level III: Vector-like Fermions and Flavor-Changing Transitions," Phys. Rev. D **102** (2020) 115015 [arXiv:2009.11296].

[120] D. Guadagnoli, M. Reboud, and P. Stangl, "The Dark Side of 4321," JHEP **10** (2020) 084 [arXiv:2005.10117].

[121] M. J. Dolan, T. P. Dutka, and R. R. Volkas, "Lowering the scale of Pati-Salam breaking through seesaw mixing," JHEP **05** (2021) 199 [arXiv:2012.05976].

[122] S. F. King, "Twin Pati-Salam theory of flavour with a TeV scale vector leptoquark," JHEP **11** (2021) 161 [arXiv:2106.03876].

[123] S. Iguro, J. Kawamura, S. Okawa, and Y. Omura, "TeV-scale vector leptoquark from Pati-Salam unification with vectorlike families," Phys. Rev. D **104** (2021) 075008 [arXiv:2103.11889].

[124] S. Iguro, J. Kawamura, S. Okawa, and Y. Omura, "Importance of vector leptoquark-scalar box diagrams in Pati-Salam unification with vector-like families," JHEP **07** (2022) 022 [arXiv:2201.04638].

[125] J. Heeck and D. Teresi, "Pati-Salam explanations of the B-meson anomalies," JHEP **12** (2018) 103 [arXiv:1808.07492].

[126] D. Marzocca, "Addressing the B-physics anomalies in a fundamental Composite Higgs Model," JHEP **07** (2018) 121 [arXiv:1803.10972].

[127] D. Marzocca and S. Trifinopoulos, "Minimal Explanation of Flavor Anomalies: B-Meson Decays, Muon Magnetic Moment, and the Cabibbo Angle," Phys. Rev. Lett. **127** (2021) 061803 [arXiv:2104.05730].

[128] D. Bečirević, *et al.*, "Scalar leptoquarks from grand unified theories to accommodate the *B*-physics anomalies," Phys. Rev. D **98** (2018) 055003 [arXiv:1806.05689].

[129] K. S. Babu, P. S. B. Dev, S. Jana, and A. Thapa, "Unified framework for *B*-anomalies, muon $g - 2$ and neutrino masses," JHEP **03** (2021) 179 [arXiv:2009.01771].

[130] T. Faber, *et al.*, "A unified leptoquark model confronted with lepton non-universality in *B*-meson decays," Phys. Lett. B **787** (2018) 159–166 [arXiv:1808.05511].

[131] T. Faber, *et al.*, "Collider phenomenology of a unified leptoquark model," Phys. Rev. D **101** (2020) 095024 [arXiv:1812.07592].

[132] L. Di Luzio, M. Kirk, A. Lenz, and T. Rauh, "ΔM_s theory precision confronts flavour anomalies," JHEP **12** (2019) 009 [arXiv:1909.11087].

[133] L. Calibbi, A. Crivellin, and T. Li, "Model of vector leptoquarks in view of the *B*-physics anomalies," Phys. Rev. D **98** (2018) 115002 [arXiv:1709.00692].

[134] A. Crivellin, D. Müller, and F. Saturnino, "Flavor Phenomenology of the Leptoquark Singlet-Triplet Model," JHEP **06** (2020) 020 [arXiv:1912.04224].

[135] **CMS** Collaboration, "Search for heavy neutrinos and third-generation leptoquarks in hadronic states of two τ leptons and two jets in proton-proton collisions at $\sqrt{s} = 13$ TeV," JHEP **03** (2019) 170 [arXiv:1811.00806].

[136] **ATLAS** Collaboration, "Searches for third-generation scalar leptoquarks in $\sqrt{s} = 13$ TeV pp collisions with the ATLAS detector," JHEP **06** (2019) 144 [arXiv:1902.08103].

[137] **ATLAS** Collaboration, "Search for pair production of third-generation scalar leptoquarks decaying into a top quark and a τ-lepton in *pp* collisions at $\sqrt{s} = 13$ TeV with the ATLAS detector," JHEP **06** (2021) 179 [arXiv:2101.11582].

[138] E. E. Jenkins, A. V. Manohar, and M. Trott, "Renormalization Group Evolution of the Standard Model Dimension Six Operators II: Yukawa Dependence," JHEP **01** (2014) 035 [arXiv:1310.4838].

[139] R. Alonso, E. E. Jenkins, A. V. Manohar, and M. Trott, "Renormalization Group Evolution of the Standard Model Dimension Six Operators III: Gauge Coupling Dependence and Phenomenology," JHEP **04** (2014) 159 [arXiv:1312.2014].

[140] M. González-Alonso, J. Martin Camalich, and K. Mimouni, "Renormalization-group evolution of new physics contributions to (semi)leptonic meson decays," Phys. Lett. B **772** (2017) 777–785 [arXiv:1706.00410].

[141] J. Aebischer, A. Crivellin, and C. Greub, "QCD improved matching for semileptonic B decays with leptoquarks," Phys. Rev. D **99** (2019) 055002 [`arXiv:1811.08907`].

[142] R. Barbieri, G. R. Dvali, and L. J. Hall, "Predictions from a U(2) flavor symmetry in supersymmetric theories," Phys. Lett. B **377** (1996) 76–82 [`hep-ph/9512388`].

[143] R. Barbieri, L. J. Hall, and A. Romanino, "Consequences of a U(2) flavor symmetry," Phys. Lett. B **401** (1997) 47–53 [`hep-ph/9702315`].

[144] R. Barbieri, G. Isidori, J. Jones-Perez, P. Lodone, and D. M. Straub, "$U(2)$ and Minimal Flavour Violation in Supersymmetry," Eur. Phys. J. C **71** (2011) 1725 [`arXiv:1105.2296`].

[145] R. Barbieri, P. Campli, G. Isidori, F. Sala, and D. M. Straub, "B-decay CP-asymmetries in SUSY with a $U(2)^3$ flavour symmetry," Eur. Phys. J. C **71** (2011) 1812 [`arXiv:1108.5125`].

[146] R. Barbieri, D. Buttazzo, F. Sala, and D. M. Straub, "Flavour physics from an approximate $U(2)^3$ symmetry," JHEP **07** (2012) 181 [`arXiv:1203.4218`].

[147] G. Blankenburg, G. Isidori, and J. Jones-Perez, "Neutrino Masses and LFV from Minimal Breaking of $U(3)^5$ and $U(2)^5$ flavor Symmetries," Eur. Phys. J. C **72** (2012) 2126 [`arXiv:1204.0688`].

[148] R. Barbieri, G. Isidori, A. Pattori, and F. Senia, "Anomalies in B-decays and $U(2)$ flavour symmetry," Eur. Phys. J. C **76** (2016) 67 [`arXiv:1512.01560`].

[149] J. Fuentes-Martín, G. Isidori, J. Pagès, and K. Yamamoto, "With or without U(2)? Probing non-standard flavor and helicity structures in semileptonic B decays," Phys. Lett. B **800** (2020) 135080 [`arXiv:1909.02519`].

[150] M. Fernández Navarro and S. F. King, "B-anomalies in a twin Pati-Salam theory of flavour." `arXiv:2209.00276`.

[151] C. H. García-Duque, J. H. Muñoz, N. Quintero, and E. Rojas, "Extra gauge bosons and lepton flavor universality violation in Υ and B meson decays," Phys. Rev. D **103** (2021) 073003 [`arXiv:2103.00344`].

[152] C. H. García-Duque, J. M. Cabarcas, J. H. Muñoz, N. Quintero, and E. Rojas, "Singlet vector leptoquark model facing recent LHCb and BABAR measurements." `arXiv:2209.04753`.

[153] S. Descotes-Genon, S. Fajfer, J. F. Kamenik, and M. Novoa-Brunet, "Testing lepton flavor universality in $\Upsilon(4S)$ decays," Phys. Rev. D **103** (2021) 113009 [`arXiv:2104.06842`].

[154] M. Beneke, *et al.*, "Leptonic decay of the $\Upsilon(1S)$ meson at third order in QCD," Phys. Rev. Lett. **112** (2014) 151801 [`arXiv:1401.3005`].

[155] **CLEO** Collaboration, "First Observation of Upsilon(3S) —> tau+ tau- and Tests of Lepton Universality in Upsilon Decays," Phys. Rev. Lett. **98** (2007) 052002 [`hep-ex/0607019`].

[156] R. Van Royen and V. F. Weisskopf, "Hadron Decay Processes and the Quark Model," Nuovo Cim. A **50** (1967) 617–645. [Erratum: Nuovo Cim.A 51, 583 (1967)].

[157] D. Y. Bardin and G. Passarino, *The standard model in the making: Precision study of the electroweak interactions.* Clarendon Press, 1999.

[158] S. Matsuzaki, K. Nishiwaki, and K. Yamamoto, "Simultaneous interpretation of K and B anomalies in terms of chiral-flavorful vectors," JHEP **11** (2018) 164 [`arXiv:1806.02312`].

[159] A. Ishikawa. Private communication.

[160] **LHCb** Collaboration, "Observation of the decay $\Lambda_b^0 \to \Lambda_c^+ \tau^- \overline{\nu}_\tau$," Phys. Rev. Lett. **128** (2022) 191803 [`arXiv:2201.03497`].

[161] **DELPHI** Collaboration, "Measurement of the Lambda0(b) decay form-factor," Phys. Lett. B **585** (2004) 63–84 [`hep-ex/0403040`].

[162] F. U. Bernlochner, Z. Ligeti, D. J. Robinson, and W. L. Sutcliffe, "Precise predictions for $\Lambda_b \to \Lambda_c$ semileptonic decays," Phys. Rev. D **99** (2019) 055008 [`arXiv:1812.07593`].

[163] F. U. Bernlochner, Z. Ligeti, M. Papucci, and D. J. Robinson, "Interpreting LHCb's $\Lambda_b \to \Lambda_c \tau \bar{\nu}$ measurement and puzzles in semileptonic Λ_b decays," Phys. Rev. D **107** (2023) L011502 [`arXiv:2206.11282`].

[164] M. Fedele, *et al.*, "Impact of $\Lambda_b \to \Lambda_c \tau \nu$ measurement on New Physics in $b \to c\, l\, \nu$ transitions." `arXiv:2211.14172`.

[165] W. Buchmuller, R. Ruckl, and D. Wyler, "Leptoquarks in Lepton - Quark Collisions," Phys. Lett. B **191** (1987) 442–448. [Erratum: Phys.Lett.B 448, 320–320 (1999)].

[166] A. Angelescu, D. Bečirević, D. A. Faroughy, and O. Sumensari, "Closing the window on single leptoquark solutions to the B-physics anomalies," JHEP **10** (2018) 183 [`arXiv:1808.08179`].